PHYSICAL AND MECHANICAL PROPERTIES OF CHICKEN FEATHER MATERIALS

A Thesis
Presented to
The Academic Faculty

by

Jeffrey W. Kock

In Partial Fulfillment
of the Requirements for the Degree
Master of Science in the
School of Civil and Environmental Engineering

Georgia Institute of Technology
May, 2006

PHYSICAL AND MECHANICAL PROPERTIES OF CHICKEN FEATHER MATERIALS

Approved by:

Dr. K. E. Kurtis, Co-advisor
School of Civil and Environmental Engineering
Georgia Institute of Technology

Dr. T. R. Gentry, Co-advisor
College of Architecture
Georgia Institute of Technology

Dr. H. Nanko
Institute of Paper Science and Technology
Georgia Institute of Technology

Date Approved: April 7, 2006

ACKNOWLEDGEMENTS

I would like to express my gratitude for the energy freely given by the many individuals who have made this research possible. I would first like to thank my co-advisors for their many helpful insights, and especially Dr. Kimberly Kurtis for her great attitude and dedication to helping me to make this document what it is. I extend thanks to Dr. Russell Gentry for sharing his humor and wisdom regarding many things. I am grateful to Dr. Hiroki Nanko, and especially the U.S. Poultry & Egg Poultry Protein & Fat Council and John Starkey for providing this research opportunity.

I greatly appreciate the time donated to this project by Ron Barbieri, as well as my original officemates Ben Mohr and Joy Justice. The good times have continued, and I have officemates Marcus Millard, Victor Garas, and Reen Foley to thank for this, as well as my roommate Daniel Baron.

Finally, I wish to acknowledge the love and gracious support provided by Holly Clark and my family – Ron and Nancy Kock as well as Adam and Ellen Koehler.

TABLE OF CONTENTS

LIST OF TABLES

LIST OF FIGURES

SUMMARY

Materials derived from chicken feathers could be used advantageously in composite building material applications. Such applications could potentially consume the five billion pounds of feathers produced annually as a by-product of the U.S. poultry industry. To aid the development of successful applications for chicken feather materials (CFM), the physical and mechanical properties of processed CFM have been characterized in this research. Results describing the moisture content, aspect ratio, apparent specific gravity, chemical durability, Young's modulus, and tensile strength for processed CFM and specifically their fiber and quill components are presented herein.

Processed chicken feather fiber and quill samples were found to have similar moisture contents in the range of 16 - 20%. The aspect ratio (i.e., length/diameter) of samples were found to be in the range of 30 - 50, and the fiber material was found to have a larger aspect ratio than the quill material. A comparison with values in the literature suggests that different processing regimes produce CFM with higher aspect ratios. Samples were found to have apparent specific gravities in the range of 0.7 - 1.2, with the fiber material having a higher apparent specific gravity than the quill material. A comparison with values in the literature suggests that apparent specific gravity results vary with fiber length and approach the value for keratin as fiber length decreases and internal voids become increasingly accessible. Chemical durability results showed that CFM rapidly degrade in highly alkaline (pH=12.4) environments and are, thus, likely incompatible with cement-based materials without special treatment.

The Young's modulus of processed chicken feather materials was found to be in the range of 3 - >50 GPa and, thus, comparable to the Young's moduli of other natural

fibers. The tensile strength of oven-dried samples was found to be in the range of 10 - >70 MPa. In agreement with results in the literature, the fiber material was found to have a greater tensile strength than the quill material. Finally, a simplified approach for comparing the effective Young's moduli and effective tensile strengths of various processed CFM samples was introduced.

CHAPTER 1

INTRODUCTION

Currently, the 4 billion pounds of chicken feathers produced annually in the United States are principally consumed by the feather meal industry, which utilizes the feather material in livestock feed [Winandy *et al*., 2003]. The development of alternative industry consumers of chicken feathers may increase the value of these feathers, which are currently valued at approximately $250/ton when sold for feather meal [Gentry *et al*., 2004]. As well, new applications will provide alternatives to landfilling of the material at a cost of $30/ton, should government regulation inspired by public concerns about bovine spongiform encephalopathy and avian influenza jeopardize the feather meal industry [GEP, 2000]. The FDA and USDA recently solicited comments and scientific opinion on "prohibiting the use of all mammalian and poultry protein in ruminant feed" [FDA, 2004]. This suggests that feather meal may not always be approved for use in feed. In the European Union, for example, poultry feather meal has been banned since 2001 [European Parliament, 2004].

Chicken feathers possess unique properties - including low relative density and good thermal and acoustic insulating properties- which could be used advantageously in a number of applications which would serve as alternatives to feather meal and feather disposal. In addition, technologies for processing chicken feathers into fibrous (feather fiber) and particulate (quill) fractions have been developed and patented (United States Patent Application 20020079074 and United States Patent 5705030) [Griffith, 2002; Gassner III, 1998]. However, although a number of commercial applications have been

investigated, market mechanisms have failed to produce alternative *high volume* consumers of the processed materials. While a nutraceutical product from feather protein has been marketed, it is unlikely that the nutraceutical industry could be an adequately high volume consumer [Barrodale, 2000]. Composite building materials containing chicken feather materials (CFM) are high volume applications which could potentially consume all of the chicken feathers produced annually in the United States and raise their market value. Based upon processing costs and the price of similar fibers, Walter Schmidt has estimated that feather fiber could yield a profit of $1000/ton [McGovern, 2000].

In order to successfully develop applications for chicken feathers in the realm of composite building materials, the physical and mechanical properties and chemical durability of CFM must first be understood. While some properties of the feather fiber fraction have previously been reported, this research comprehensively quantifies these basic material properties for both processed feather fiber and quill. The moisture contents, aspect ratios, and specific gravities of feather fiber and quill are evaluated and compared with previously reported values. The chemical durability of feather fiber and quill in alkaline, near-neutral, and slightly acidic solutions is measured and compared with previously reported observations. The moduli of elasticity and tensile strengths of feather fiber and quill are also measured and compared with previously reported values. This data can be used to target applications and to develop financial analyses informed by an understanding of necessary processing costs and potential financial benefits.

Chapter II consists of a literature review of chicken feather properties, processed feather fractions and their potential applications, and also analytical models used to

derive the mechanical properties of CFM from those of composites reinforced with CFM. Sample materials and experimental methods are discussed in Chapter III. Chapter IV contains the research results and a discussion of all data. Finally, Chapter V presents conclusions, suggestions for future fundamental property studies, and suggestions for the development of successful composite applications for CFM based upon the results presented herein.

CHAPTER II

LITERATURE REVIEW

2.1 General Information

2.1.1 Chicken Feathers

Feathers distinguish birds from other vertebrates and play an important role in numerous physiological and functional processes. Most adult birds are covered entirely with feathers, except on the beak, eyes, and feet. Feathers not only confer the ability of flight, but are essential for temperature regulation. Feathers are highly ordered, hierarchical branched structures, ranking among the most complex of keratin structures found in vertebrates [Yu, 2002].

Chicken feathers are approximately 91% protein (keratin), 1% lipids, and 8% water [Lederer]. The amino acid sequence of a chicken feather is very similar to that of other feathers and also has a great deal in common with reptilian keratins from claws [Fraser, 1996]. The sequence is largely composed of cystine, glycine, proline, and serine, and contains almost no histidine, lysine, or methionine [Schmidt, 1998].

When hatched, a chick is covered with natal down and soon a "first feathering" begins to appear. These immature feathers are small, lack color, and show no sexual variation. A second set of plumage begins to replace the first at 2-3 weeks, and by about the fourth month, a chicken's feathers are again replaced. The animal has then reached sexual maturity [Anatomy].

Feather follicles are arranged in rows or tracts. A follicle may produce many feathers over the course of a chicken's lifetime. Shedding or molting usually occurs twice

a year, but may be as infrequent as once every two years, depending on environment, age, food source, and other factors. Feathers can also regrow to replace those lost through injury [Anatomy].

There are five commonly recognized categories of feathers: contour, down, semiplume, filoplume, and bristle. However, Schmidt and Line [1996] report that differences in keratin organization result in approximately 30 macroscopically distinct poultry feather types. Information about the common feather categories is presented below.

Contour, or vaned, feathers give birds their color and provide the first layer of defense against physical objects, sunlight, wind, and rain. Contour feathers are found on a bird's back, tail, and wings, and are primarily responsible for flight. Each contour feather has a feather shaft and a flat vane extending from it [Bartels, 2003]. The naked portion of the shaft that is implanted in a bird's skin is the calamus. The portion bearing branches is the rachis, which is filled with a porous substance termed the medulla. Branches are termed barbs and provide an axis from which barbules can branch. Barbules are very closely spaced and interlock via hooklets, or barbicels, in order to provide strength and repel water. Flightless birds, including the emu and the ostrich, have few, if any, hooklets [Lederer]. Thus, it can be assumed that hooklets are not abundant in chickens. A typical contour feather is diagrammed in Figure 2.1 and depicted in Figure 2.2a.

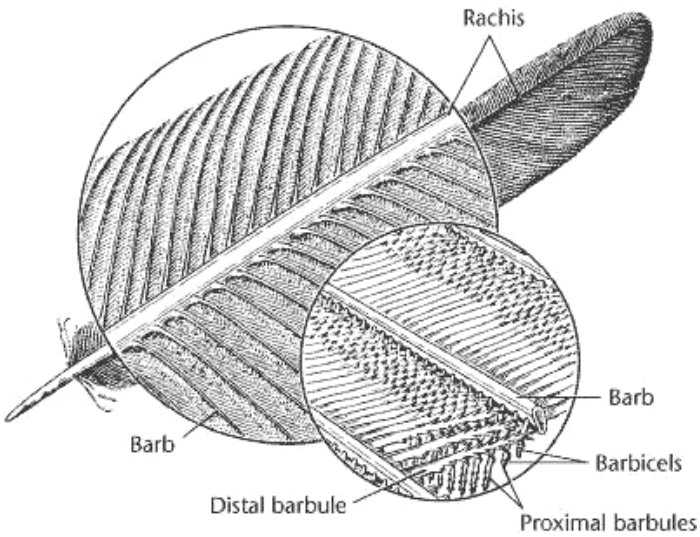

Figure 2.1 A contour feather [Bartels, 2003].

Down feathers are smaller than contour feathers and lack barbules and the accompanying hooklets. They are soft and fluffy, located beneath the contour feathers. They provide most of a chicken's insulation. There are several subcategories of down, including natal down, present only at hatching, and powder down, which is a specialized feather type that sheds a fine, white keratin powder. The waxy powder is composed of granules so small that it is unwettable and thus forms a waterproof barrier for contour feathers [Lederer, Anatomy]. A powder down feather is depicted in Figure 2.2d.

The semiplume (Figure 2.2c) is a feather type that mediates between the categories of contour and down. Semiplumes share characteristics with both; they have a large rachis and predominantly downy vanes. Filoplumes (Figure 2.2e) are smaller than semiplumes, with only a few barbs at the tip of a fine shaft. These likely serve a sensory function in chickens, registering vibrations and changes in pressure. The smallest type of feather is the bristle, which is stiff and has few, if any, short barbs near the tip. Bristles (Figure 2.2b) are protective in function and are found on a chicken's head, at the base of the beak, around the eyes, and covering the nostrils [Lederer, Anatomy].

According to engineering staff at the Gold Kist chicken processing plant in Carrollton, Georgia, a plant might process chickens of different sizes on different days. Differently-sized chickens, presumably of different ages, could be expected to yield different distributions of these feather types. For example, some smaller chickens have mostly downy feathers, while older and larger chickens would be expected to have relatively more contour feathers. Thus, chicken feather properties could vary by collection day. In order to maximize the yield of a desirable type of feathers, feather collection could be planned for days on which chickens of a particular feather type distribution are processed.

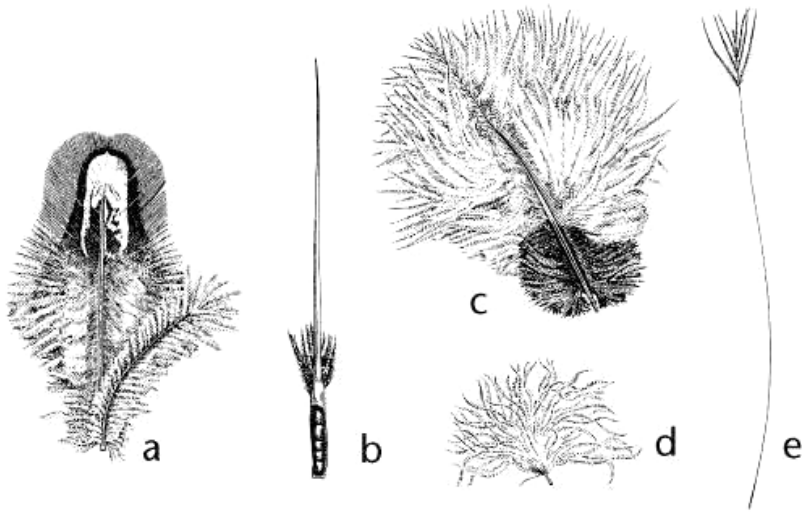

Figure 2.2 The five primary types of chicken feathers: (a) contour, (b) bristle, (c) semiplume, (d) down, (e) filoplume [Bartels, 2003].

2.1.2 Processed Chicken Feather Fractions

Large contour feathers are approximately half feather fiber and half quill by mass [Winandy *et al.*, 2003]. These are useful categories because several companies' proprietary processing technologies yield these two fractions, fiber and quill, shown in Figure 2.3. Also, Hong and Wool [2005] assert that fiber keratin and quill keratin are

characteristic of the two forms of microcrystalline keratin in feathers. In simple terms, the quill is the hard, central axis off which soft, interlocking fibers branch. The fibers are hollow [Hong and Wool, 2005]. Smaller feathers have a greater proportion of fiber, which has a higher aspect ratio than the quill [Winandy, 2003], as is apparent in Figure 2.3. A single keratin fiber has a maximum diameter of 50 μm [Misra, 2001]. Quill fractions are composed of both inner and outer quill; outer quill is more densely structured than inner quill, which is porous, as is apparent in Figure 2.3. Gassner *et al.* [1998] have reported that the presence of quill among fibers results in a more granular, lightweight, and bulky material. A typical quill has dimensions on the order of centimeters (length) by millimeters (diameter). Figure 2.3 shows scanning electron micrographs of outer quill (c), inner quill (d), and fiber (e).

Hong and Wool [2005] report that the thermal energy required to perturb the fiber is higher than that required to perturb the quill. Schmidt and Line [1996] suggest that the packing within outer quill keratin is less ordered and/or has less cross-linking than packing within fiber and inner quill keratin. Thus, it is the outer quill component of a quill fraction which is weaker. Outer quill would be weakened by mechanical stresses that the feather fiber and inner quill would be able to withstand.

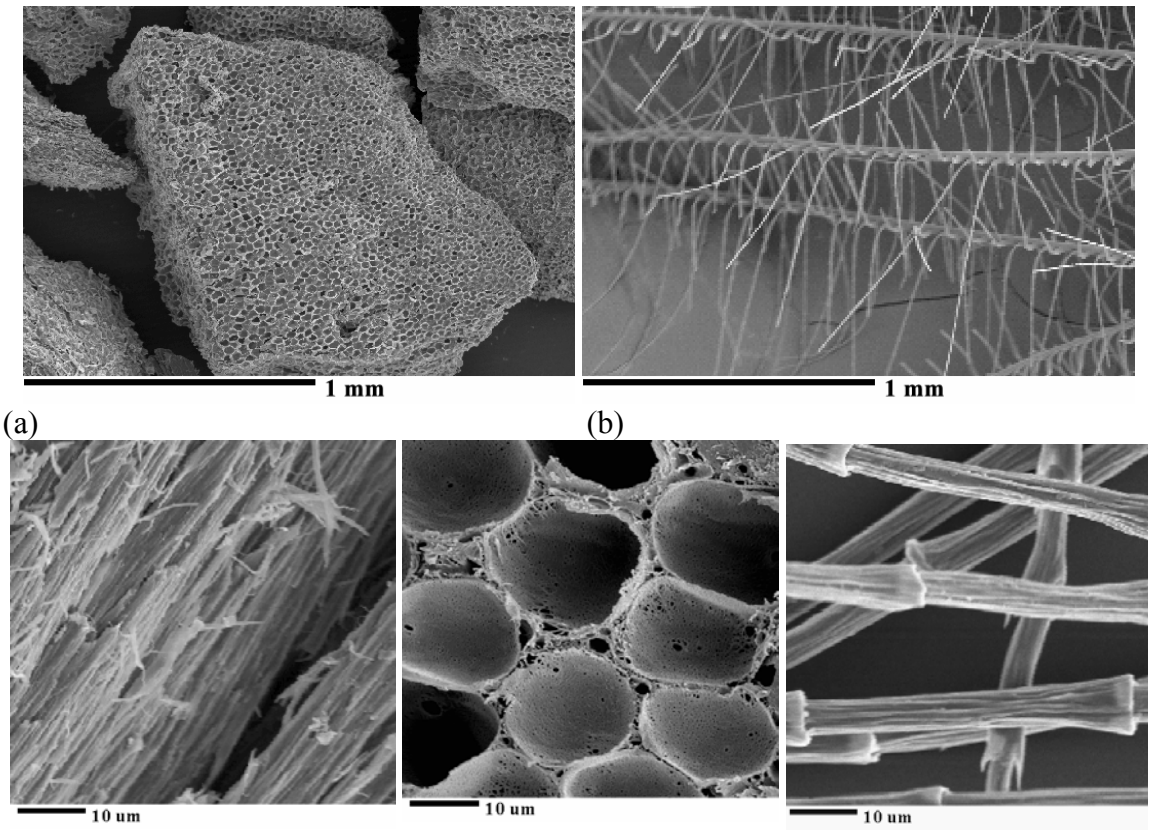

Figure 2.3 Scanning electron micrographs showing chicken feather (a) inner quill, (b) fiber, (c) outer quill, (d) inner quill, and (e) fiber.

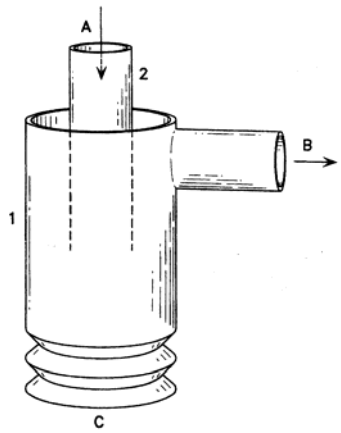

Figure 2.4 Turbulent flow chamber for feather separation [Gassner *et al*., 1998].

Walter Schmidt and his colleagues at the United States Department of Agricultural (USDA) developed and patented a fiber and quill separation process that

utilizes turbulent air flow [Gassner et al., 1998]. The chicken feathers are cleaned with a polar solvent, like ethanol, and are dried. A high precision shredder then minces the whole feathers and the resulting particles are passed down a small cylindrical tube (Figure 2.4-2). A larger tube (Figure 2.4-1), with air flowing up the inside of it, creates turbulent flow at the end of the smaller, inner tube. Under such conditions, the large quill particles fall to the bottom of the column and can be removed while the lighter and smaller fiber fraction continues to be suspended.

2.1.3 Applications

Recent interest in investigating alternative uses for CFM has spawned a number of potential applications. Knowledge of applications under investigation provides a context for the study of the fundamental properties of CFM and motivates the study of certain properties in particular. The use of CFM as a contaminant adsorbent is one current area of research. Others are investigating CFM in applications that take advantage of its electrical conductance and insulating properties. Paper, erosion control fabrics, and composite applications for CFM are other uses under investigation.

Adsorption is one of the most important methods for cleaning industrial effluents, and keratin protein can act as a fibrous, nano-filtering sponge. The fiber fraction of chicken feathers has a high surface area (12 m^2/g, as measured by BET) and partially hollow medulla structure due to a network of 0.05-0.10 μm nanopores. Combined with the appropriate active functional groups, this endows feathers with the unique and valuable capacity to bind and thereby remove heavy metals from wastewater. Misra et al. [Misra et al., 2001] discovered that metal uptake is sensitive to pH, temperature, and the amount of keratin fiber used. The binding process is rapid, and the metal cations most

effectively removed by feather fiber are chromium, copper, lead, mercury, nickel, and zinc.

Al-Asheh et al. [Al-Asheh et al., 2003] compared the binding properties of natural feathers to chemically-activated feathers, treating a group of feathers with alkaline solutions of NaOH and Na_2S and another group with sodium dodecyl sulfate (SDS), an anionic surfactant. This research confirmed that non-activated feathers are effective at removing both copper and zinc from solution. The feathers treated with SDS performed better, and those activated with alkaline solutions were the best adsorbers, binding nearly twice as much zinc as the untreated feathers when exposed to a high concentration.

Another proposed application for chicken feathers is in computer chips. Wool and Hong [2004] are prototyping a new generation of microchips that use CFM to replace silicon. Because of their strength and because their porous structure is filled with air, feathers are good conductors of electrons, which makes them suitable for this application. Circuit boards produced with feather material are approximately 50% lighter and that electrical signals move twice as quickly through a feather fiber chip when compared with a conventional silicon chip [Barnes, 2002; Jacobson, 2002].

Ye and Broughton [1999] created a nonwoven insulation (batting) from chicken feather fiber and a small amount of binder fiber. The insulating properties of this batting were compared with those of batting made from goose down and batting from polyester fibers. The filling power, or volume a given weight of material will occupy under a standard pressure, was measured for each batting. Filling power can be correlated to thermal insulating quality for batting. By this measure, chicken feather batting exhibited

better insulating properties than polyester fibers, but did not perform as well as goose down.

Fiber from chicken feathers has been fabricated into an assortment of paper products. Decorative paper has been created with an unusual texture and dyeing properties. Because this chicken feather composite paper is made of 51% feather fiber and 49% wood pulp, only half as many trees are needed to produce it [Durham, 2002].

Geo-fabrics for erosion control have been developed from latex-bonded non-woven turkey feather material. When compared to traditional products made of jute and coconut, the turkey feather fabrics performed similarly in terms of light and water transmittance. The feather fabrics did not affect pH, nitrogen, or phosphorous content of the soil, and actually increased moisture content while decreasing compaction [George *et al*., 2003a].

A variety of studies have investigated the influence of chicken feather fiber inclusion on composite properties. Winandy *et al.* [2003] studied aspen fiber medium density fiberboard composite panels with feather fiber replacement in amounts ranging from 20% to 95%. 5% phenol formaldehyde was used as an adhesive. Compared with 0% chicken feather fiber panels (95% aspen fiber), the 47.5% chicken feather fiber panels demonstrated 27% loss in modulus of elasticity and 18% loss in bending strength. The 95% chicken feather fiber panels demonstrated 51% loss in modulus of elasticity and 39% loss in bending strength. The feather fiber panels showed a significant improvement in resistance to water absorption, associated thickness swell, and mold growth, probably due to the hydrophobic elements in keratin's amino acid sequence. Compared with 0% chicken feather fiber panels, the 47.5% chicken feather fiber panels demonstrated 38% 2-

hour thickness swell and 48% water absorption. The 95% chicken feather fiber panels demonstrated 27% 2-hour thickness swell and 36% water absorption. While the 0% chicken feather fiber panels experienced 65% mass loss due to brown rot (BR) and 47% due to white rot (WR), the 47.5% chicken feather fiber panels experienced 6% (BR) and 11% (WR) mass loss, and the 95% chicken feather fiber panels experienced 16% (BR) and 20% (WR) mass loss.

Dweib *et al.* [2004] fabricated composite sandwich beams made from all natural materials. The team's goal was to develop 100% natural monolithic structural members suitable for use in load-bearing roofs, floors, or walls of residential and commercial units. Bio-based thermoset resins made from plant oils (soybean) were used, and the effects of different natural fibers, including flax, cellulose, recycled paper, and chicken feather fiber, were investigated. Chicken feather fiber mats provided by Tyson were used. These were composed of 97% feather fiber and 3% low molecular weight polymeric binder. Dweib *et al.* used Vacuum Assisted Resin Transfer Molding (VARTM), a very clean and economical manufacturing approach which involves driving resin into a dry, vacuum-enclosed environment using only vacuum pressure. This results in a component with enhanced mechanical properties and low void volume. Recycled paper from corrugated cardboard boxes, used in combination with feather fiber mats, provided reinforcement to the neat resin. The compacted fiber in the cardboard imparted structural stability during processing, while the porous feather mats provided flow channels to better distribute the resin. Table 2.1 shows a comparison among the mechanical properties of wood beams and composite beams using chicken feather fiber, corrugated paper, or E-glass fiber mats to provide flow channels. The chicken feather fiber beam

performed marginally worse than the other composite beams in flexural rigidity and flexural strength. The composite beams generally performed as well or better than wood members in flexural rigidity and flexural strength, indicating that they could potentially be used in the future for structural applications.

Table 2.1 Mechanical properties of composite sandwich beams [Dweib *et al*., 2003].

Beam	Flexural Rigidity-EI ($kN\text{-}m^2$)	Strength (kN)
Composite Beams		
Recycled paper/ chicken feathers	12.4	24.2
Recycled paper/ corrugated paper	14.8	25.8
Recycled paper/ E-glass fiber	19.9	25.6
Wood Beams		
Douglas fir	18.0-30.3	15.4-29.7
Spruce	16.0-25.0	10.7-24.5
Cedar	10.0-26.4	9.5-28.8

Dweib *et al*. [2004], in another study, investigated the properties of bio-based composites containing soybean oil-based resin and hybrid natural fiber mats. The hybrid fiber mats were composed of varying percentages of chicken feather fiber, recycled kraft paper fiber, and recycled newspaper fiber and were made using a wetlay papermaking process. VARTM was used to infiltrate the fiber mats with resin. Composites were tested in tension and in 3-point bending. The fiber mats, in all cases, increased composite mechanical properties (strength and modulus) over those of the neat resin by at least a factor of 2. The neat resin had a tensile modulus of approximately 0.9 GPa. Composites with fiber mats containing 40wt% kraft paper fiber and 60wt% chicken feather fiber had a tensile modulus of approximately 2.1 GPa, while composites with fiber mats containing

40wt% kraft paper fiber, 30wt% newspaper fiber, and 30wt% chicken feather fiber had a tensile modulus of approximately 2.4 GPa.

2.2 Physical Properties

2.2.1 Moisture Content

The moisture content of CFM is an important variable that can have implications ranging from transportation costs to mechanical properties. The moisture content of processed CFM can vary depending upon processing and environmental conditions. At chicken processing facilities such as the Gold Kist facility in Carrollton, Georgia, feathers are removed from chickens using hot water and mechanical action, and the loose feathers are transported through the processing plant in a water trough. As a consequence, the feathers can be in a saturated state before they are processed. Part of the processing regime may reduce the moisture content to levels at which the feathers are thought to be biologically stable. The as-received moisture content of processed CFM may vary significantly. Kar and Misra [2004] reported that the moisture content of chicken feather fiber, provided and processed by MaXim LLC, was 12-13% in its as-received state.

Keratin can be considered to have both hydrophilic and hydrophobic properties. While 39 of the 95 amino acids in the keratin monomer are hydrophilic, serine, the most abundant amino acid, gives chicken feathers the ability to attract moisture from the air, because of the free OH^- group on the surface of each serine molecule [Alberts *et al*., 1994]. Thus, CFM may be considered to be hygroscopic.

For example, Taylor *et al.* [2004] measured the moisture content of ostrich feather rachis conditioned at 0%, 50%, and 100% relative humidity (RH). At 50% RH, the

rachis was found to have a moisture content, as a percentage of the wet mass, of 11.7%. At 100% RH, the rachis was found to have a moisture content, as a percentage of the wet mass, of 28.4%.

Conditioning CFM to particular moisture states without altering its structure requires knowledge of its basic thermal properties to avoid degrading the material. Schmidt and Line [1996] used differential scanning calorimetry (DSC) to measure thermal properties of fiber, inner quill, and outer quill fractions. By this method, a sample is heated 10°C per minute from ambient to 350°C, and the differential heat absorbed is recorded. Schmidt and Line reported that the glass transition temperature (T_g) is approximately 235°C for feather fiber and inner quill, and approximately 225°C for outer quill. According to Schmidt and Line, a higher T_g indicates a tighter keratin structure to which water is more strongly bonded. Fiber and inner quill do not begin to lose water below 100°C. After drying at 110°C overnight under vacuum, moisture was found to be fully removed from outer quill and not fully removed from inner quill and fiber. DSC work presented by Kock *et al.* [2005] showed that the moisture evolution temperature of chicken feather fiber and quill fractions occurs in the range of 100-110°C. This suggests that it may be possible to fully dry fiber and inner quill at 110°C over time.

2.2.2 Aspect Ratio

Kar and Misra [2004] measured by scanning electron microscopy the diameter of chicken down feather fibers obtained from MaXim LLC. Fiber diameters were found to be in the range of 5-50 μm.

Dweib *et al*. [2004] examined chicken feather fiber from Featherfiber Corporation. These fibers were reported to have diameters of 6-8 μm and lengths of 3-13 mm. These values correspond to aspect ratios of 400-2200. Barone and Schmidt [2005] also examined chicken feather fiber from Featherfiber Corporation. Barone and Schmidt found that fibers had a constant diameter of approximately 5 μm and lengths between 3.2 and 13 mm. These values correspond to aspect ratios of 600-2600.

Values for chicken feather fibers obtained from Tyson Foods, Inc. were reported by Hong and Wool [2005]. Hong and Wool reported typical values of 6 μm for fiber diameter, 8mm for fiber length, and 1000 for fiber aspect ratio.

2.2.3 Apparent Specific Gravity

Hong and Wool [2005] have reported that the density of chicken feather fiber, provided by Tyson Foods, Inc., is 0.8 g/cm^3. This value is interpreted as an apparent density value because it is not the weight of a voidless volume of solid matter, but instead it is the weight of a volume of both solid matter (the walls of the fiber) and air (the hollow inside the fiber). The value cited by Hong and Wool was calculated from the properties of feather fiber composites which consisted of feather fibers contained in a polymer matrix material of known properties. The value was confirmed by a density calculation considering the density and thickness of fiber walls and the fiber outside diameter [Wool, 2005]. Hong and Wool reported a typical value of 8 mm for fiber length [Hong and Wool, 2005].

Barone and Schmidt [2005] measured the density of chicken feather fiber, obtained from Featherfiber Corporation, by displacing a known volume and weight of

ethanol with an equivalent amount of fiber. They reported a value of 0.89 g/cm^3 for the chicken feather fiber. Barone and Schmidt do not comment on whether this value represents apparent density. However, because Barone and Schmidt's [2005] value of 0.89 g/cm^3 is relatively similar to Hong and Wool's [2005] cited value of 0.80 g/cm^3 when compared with a value of 1.3 g/cm^3 for the density of solid keratin [Arai *et al*., 1989], it can be assumed that Barone and Schmidt reported an apparent density. Barone and Schmidt reported fiber lengths of 3.2-13 mm.

The difference in results may be related to composition differences between the chicken feather fiber samples studied. Alternatively, Barone and Schmidt's [2005] value may be higher due to the presence of shorter fibers (as short as 3.2 mm in length). The hollows, or voids, inside chicken feather fibers may become more accessible to ethanol (in the case of Barone and Schmidt [2005]) or polymer resin (in the case of Hong and Wool [2005]) as fiber length decreases. For a fiber of some critical length, the void inside of this fiber acts as a part of its surface, and as a result only the solid matter of this fiber will be accounted for by a measurement of apparent density. Assuming a density of 1.3 g/cm^3 for the solid matter of chicken feather fiber (keratin) [Arai *et al*., 1989], apparent density results will approach 1.3 g/cm^3 as fiber length decreases.

Hong and Wool [2005] studied the bulk density of chicken feather fiber soy resin (density of 1.08 g/cm^3) matrix composites produced with the VARTM process. Composite bulk density was higher than expected (1.001 g/cm^3) for the composite containing 30wt% feather fiber. The authors concluded that the VARTM process had caused a 5% filling of the hollow keratin fibers which accounted for higher bulk

composite density. The higher bulk composite density could also be explained by a higher value for the apparent density of feather fiber.

Assuming values listed for natural fibers and glass fiber in Table 2.2 represent apparent specific gravities, then chicken feather fiber has a low apparent specific gravity (0.8-0.9), even among other natural fibers. Thus, CFM inclusion in a composite could potentially lower composite density, whereas the density of a typical composite with synthetic reinforcing increases as fiber content increases [Hong and Wool, 2005]. Thus, substantial savings, in terms of transportation and construction costs, could be derived from the use of lightweight composites containing CFM.

Saheb and Jog [1999] define specific modulus as elastic modulus divided by specific gravity. Natural fibers generally have high specific mechanical properties. This is one of the major advantages of using natural fibers for applications that benefit from weight reduction. Table 2.2 shows that jute and flax fibers both have higher values of specific modulus than glass fiber, for example. Thus, it is useful to consider the specific mechanical properties of CFM.

Table 2.2 Specific gravity and mechanical properties of natural fibers [Saheb and Jog, 1999].

Fiber	Specific Gravity	Tensile Strength (MPa)	Modulus (GPa)	Specific Modulus
Jute	1.3	393	55	38
Sisal	1.3	510	28	22
Flax	1.5	344	27	50
Glass Fiber-E	2.5	3400	72	28

2.2.4 Chemical Durability

The structure of keratin, the primary constituent of chicken feathers, affects its chemical durability. Because of extensive cross-linking and strong covalent bonding

within its structure, keratin shows good durability and resistance to degradation. Efforts to extract keratin proteins from feathers illustrate this point. Extraction is a difficult task because it can only be achieved if the disufide and hydrogen bonds are broken. Schrooyen [1999a] found keratin to be insoluble in polar solvents, such as water, as well as in nonpolar solvents. The most common method for dissolving feather keratins is solubilization with concomitant peptide bond scission via acid and alkali hydrolysis, reduction of disulfide bonds with alkaline sodium sulfide solutions, or a combination of enzymatic and chemical treatment [Schrooyen, 1999b]. Although these techniques are effective for extracting keratin (75% yield), they require extremely high reagent concentrations that are much higher than keratin fibers would ever be exposed to in nature. One can deduce from this that keratin is a relatively sturdy, stable protein.

A study by Hamoush and El-Hawary [1994] indicates incompatibility between CFM and cement based materials. They conducted a study of feather fiber reinforced concrete and investigated the influence of feather fiber reinforcement on concrete density, compressive strength, and split tensile strength. Three volume fractions of chicken feathers (1, 2, and 3%) were tested. The feathers were collected, washed, screened, and dried; the quill fraction was not separated from the fiber fraction. Chicken feathers were found to detrimentally affect the compressive and tensile strengths. These values decreased sharply with increasing fiber volume fraction. The concrete samples made with feathers showed a slight improvement in flexural strength, but only at 1% replacement. The only measurable benefit imparted by chicken feathers was a reduction in weight. The authors cite severe feather decay as a cause for the adverse effects; the

feathers were found to have severely decayed at the time of testing [Hamoush and El-Hawary, 1994].

This study may indicate that highly alkaline environments promote degradation in CFM. The pore solution in cement-based materials is strongly alkaline, with a pH of 12.5-13.5, typically [Mehta and Monteiro, 2006]. Contained CFM would have the ability to degrade if susceptible, as it would be in contact with the strongly alkaline pore solution.

A study by Kar and Misra [2004] examined solutions of various pH in order to study the influence of pH on heavy metal ion uptake by feather fiber. Solution with pHs in the range of 2-8 were found to best promote uptake. It was found that 99% of adsorbed copper ions could be desorbed by washing feather fiber with dilute hydrochloric acid at a pH of 1.2. The authors concluded that the stability of the feather fiber allows it to be reused after being submitted to washing in hydrochloric acid.

The chemical durability of CFM can be further tested by subjecting fibers to synthetic environments modeled after potential use conditions. It is typical to simulate cement-based material pore solutions with basic solutions having pHs between 12 and 13.5. While authors have used various concentrations of calcium hydroxide, sodium hydroxide, and potassium hydroxide to produce simulated pore solutions, Benmokrane *et al*. [1998] as well as Katsuki and Uomoto [1995] have used diluted sodium hydroxide alone. The duration of durability studies using simulated pore solutions typically range from 28 days to more than one year [Gentry, 2001]. Wood products can be modeled with mildly acidic synthetic environments. Most timbers are have pHs of 3-6. Pine tends to have higher pH values of 5-6 [Bootle, 1983].

2.3 Mechanical Properties

2.3.1 Young's Modulus

The mechanical properties of a bird's feathers are highly related to their function. The biophysical chemistry of feathers is optimized for avian locomotion. Feathers must bend under the aerodynamic forces generated during flight while also being very lightweight [Bonser and Purslow, 1995]. The mechanical properties of CFM are related to the structure of keratin. Keratin, like other biological polymers, possesses a structure with covalent bonds that transfer forces while only negligibly distorting. Strains are largely produced by changes in the hydrogen bonds, van der Waals, and Coulombic interactions. According to Feughelman [2002], this consistency among natural protein fibers results in similar moduli of elasticity. However, Bonser and Purslow's [1995] summary of studies since 1966 reports moduli of elasticity for feather keratin ranging from 0.045 GPa to 10 GPa. Bonser and Purslow suggest that this range could indicate a high degree of interspecific heterogeneity in keratin properties. Alternatively, differences in testing methodology could explain the range.

Bonser and Purslow [1995] performed uniaxial tension tests on 25 mm sections of keratin cut from the rachis dorsal surface of flight feathers from eight volant species that are each from a separate order. The Young's modulus was found to be approximately 2.5 GPa for all species except the grey heron (1.78 GPa). Bonser and Purslow also found the Young's modulus to increase markedly along the length of the rachis, with the highest values at the feather tip (Figure 2.5). To explain this, they considered a feather to act as a simple airfoil in a laminar flow. Since the drag profile is proportional to the thickness of

the rachis, an increase in flexural strength towards the tip would allow for a smaller shaft diameter.

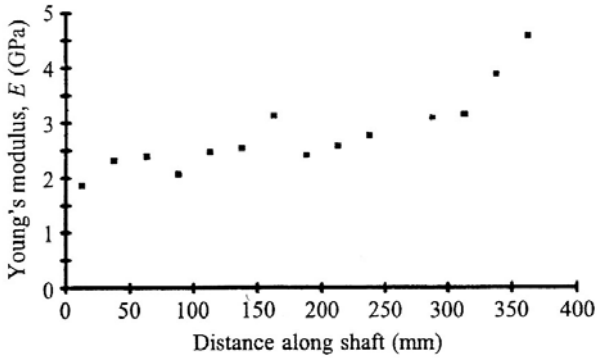

Figure 2.5 Variation in Young's modulus along the length of a mute swan's primary feather [Bonser and Purslow, 1995].

Further work by Cameron *et al.* [2003] confirmed that the mechanical properties of feather keratin vary appreciably along the length of the rachis. Using x-ray diffraction, Cameron *et al*. discovered that, moving from calamus to tip, the keratin molecules become more aligned than at the bird's skin before returning to a state of higher disorder towards the rachis tip. In this study, a terrestrial bird (ostrich) was examined, and results were compared to those for volant birds (swan and goose). The swan and goose feathers both proved to be functionally gradient, with Young's modulus varying from 2.5-3.0 GPa at the calamus to 4.5-5.0 GPa at the rachis tip. The ostrich feathers had a significantly lower modulus and did not show an increase along their length. Thus, it may be assumed that the feathers from volant birds have greater elastic moduli than feathers from terrestrial birds.

George *et al*. [2003b] studied turkey feather fiber properties for fibers at different positions along the rachis. It was found that both the tenacity and modulus of turkey feather fiber, measured in g/denier, increased with the distance from the calamus.

Turkeys are volant, though they only fly in short bursts. Thus, it appears that both the rachis and fiber material of feathers from volant birds are functionally gradient.

Purslow and Vincent [1978] measured the elastic modulus of feather rachis from pigeons, with and without inner quill. Dehydrated feather rachises were tested in bending. Elastic modulus values for the rachis with inner quill were greater than values for rachis without inner quill.

Taylor *et al*. [2004] studied the affect of moisture content on mechanical properties. Ostrich feather rachises conditioned at 0%, 50%, and 100% RH were tested in uniaxial tension at a crosshead displacement rate of 1 mm per min. The Young's modulus was calculated from the initial, linear-elastic portion of the stress-strain curves. Mechanical testing results, presented in Table 2.3, suggest that increasing moisture content decreases rachis Young's modulus. At 50% RH, the rachis was found to have a Young's modulus of 2.6 GPa. Schmidt and Line suggest that for feather fiber, the helical state of the keratin becomes more strongly bound as water is removed, giving a higher stiffness [Schmidt and Line, 1996].

Table 2.3 Mechanical properties of ostrich feather rachis [Taylor *et al*., 2004].

Mechanical Property	0% RH	50% RH	100% RH
Young's Modulus (GPa)	3.66	2.58	1.47
Tensile Stress at Failure (MPa)	221	130	106.3
Strain at Failure (%)	9.2	10.4	16.3

2.3.2 Tensile Strength

Naresh *et al*. [1991] measured the tensile strength of human hair, which is composed of keratin. The hair was mounted on cardboard and tested at a strain rate of

50% per min. Hairs of length 2 cm were tested at 65% and 100% RH. The tensile strength of the hairs at 65% RH was 180 MPa, while the tensile strength of the hairs at 100% RH was 143 MPa. This suggests that tensile strength, like elastic modulus, varies indirectly with moisture content.

It is important to note that mammalian keratin differs from avian keratin and therefore may exhibit different mechanical properties. While Naresh *et al*. reported that human hair contains an α-helical polypeptide, feather keratin can contain both α-helical and β-sheet conformations. Chicken feather fiber primarily consists of α-helical conformations, and some β-sheet conformations are present. Chicken feather outer quill consists almost entirely of β-sheet conformations, and few α-helical conformations are present [Schmidt and Jayasundera, 2003]. Hard β-sheet keratins have a much higher cystine content than soft α-helix keratins and thus a much greater presence of disulfide (S-S) chemical bonds which link adjacent keratin proteins (Figure 2.6). These strong covalent bonds stabilize the three-dimensional protein structure and are very difficult to break [Alberts *et al*., 1994]. This suggests that chicken feather outer quill would be stronger than chicken feather fiber. However, a study of the thermal properties of chicken feather fractions by Schmidt and Line [1996] suggests that outer quill is weaker than fiber and inner quill.

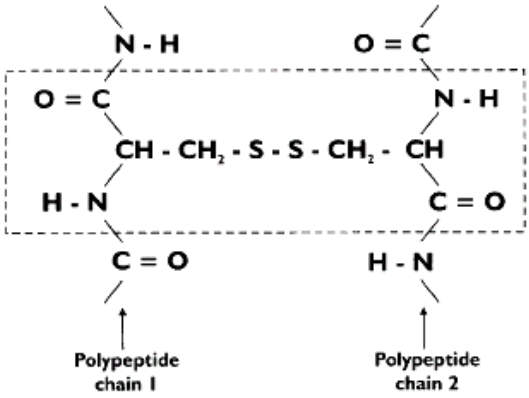

Figure 2.6 Diagrammatic representation of the diamino-acid cystine residue linking two polypeptide chains by covalent bonding [Feughelman, 2002].

Mechanical property test results for ostrich contour feather rachis, presented by Taylor *et al.* [2004] and shown in Table 2.3, give rachis tensile strength and strain at failure as a function of moisture content. The tensile strength of feather rachis conditioned at 100% relative humidity was 106 MPa. The tensile strength of feather rachis conditioned at 0% relative humidity was 221 MPa. Results show that tensile strength varies indirectly with moisture content. Alternatively, strain varies directly with moisture content.

Fraser and MacRae [1980] reported similar results for feathers from the volant Laysan albatross. At 100% RH, peak stress was measured as 100 MPa. At 65% RH, peak stress was measured as 200 MPa. It can be assumed that at 0% RH, the peak stress would be greater than 221 MPa. It is consistent with the findings of Cameron *et al*. [2003] that the tensile strengths of feathers from volant birds (albatross) are greater than those of feathers from non-volant birds (ostrich). It was shown by Cameron *et al*. that elastic modulus values are higher for volant birds than for non-volant birds.

Hong and Wool [2005] have measured the tensile fracture strength of chicken feather fiber directly. Fibers were held by adhesive tape and tested in tension with a

crosshead speed of 1.3 mm/min. Fiber diameter was measured with an optical microscope and used to determine fiber area. They reported that strength results varied due to the heterogeneity of the fibers. Strengths ranged from 41-130 MPa. Hong and Wool also calculated fiber strength from experimentally derived fracture energy data for a feather fiber reinforced composite. The calculated results of 94-187 MPa agree well with the directly measured strength results.

2.3.3 Testing Particle-Reinforced Composites

Direct and accurate measurements of the bulk mechanical properties of heterogeneous, short fiber materials (particles) such as processed CFM are challenging to obtain, particularly when a large portion of the particles are too short for direct tensile testing, as is often the case with processed CFM. One way to indirectly determine bulk properties is to derive reinforcement properties from those of a composite reinforced with the material of interest. Appropriate analytical models must be selected for the calculation of particle properties. These are reviewed herein.

2.3.3.1 Young's Modulus Analytical Models

Numerous analytical models may be used to predict composite Young's modulus as a function of composition and particle and matrix properties. Simple models readily describe unidirectional continuous fiber composites, whereas more sophisticated models must be employed to describe properties of randomly oriented short fiber (particle) composites.

The following simple rule of mixtures:

$$E_C = (1 - v_F)E_M + v_F E_F \qquad \text{Equation 2.1}$$

relates composite elastic modulus (E_C), matrix modulus (E_M), longitudinal particle elastic modulus (E_F), and particle volume fraction (v_F). This equation was developed for unidirectional continuous fiber composites from an assumption of strain compatibility in the particles and matrix. This model assumes the matrix material to be isotropic and neglects Poisson effects. If stress compatibility were instead assumed to exist in the particles, matrix, and composite, Equation 2.2 would apply:

$$\frac{1}{E_C} = \left(\frac{1 - v_F}{E_M}\right) + \frac{v_F}{E_F} \qquad \text{Equation 2.2}$$

This equation is sometimes used to predict transverse composite elastic modulus. However, the assumption of equal stresses in the constituents is rarely valid, because actual particle-packing arrangement rarely causes stresses to be equal [Gibson, 1994].

Table 2.4 Young's modulus (E), tensile strength (T), and elongation (e) are substantially affected as particle orientation increases from random (Sample 1) to aligned (Sample 5) [Goettler, 2001].

Sample	E_2/E_1	T_2/T_1	e_1/e_2
1	1.1	1.1	1.0
2	3.3	1.9	2.0
3	5.0	2.1	3.1
4	5.8	2.3	3.8
5	14.6	2.1	7.0

Particle orientation and length substantially affect composite mechanical properties. A discontinuous fiber (particle) composite is not as strong or stiff as a continuous fiber composite, when the composites are otherwise the same. However, particle orientation is more important than particle length in the determination of composite elastic modulus [Gibson, 1994]. It can be shown (Table 2.4) that increasing

particle alignment more affects elastic modulus than tensile strength. Christensen and Waals [1972] were the first to develop a model to describe the elastic modulus of a composite with particles randomly oriented in three dimensions. This model uses a spherical coordinate system to express E_C in terms of five independent engineering constants. Cox [1951] had previously developed the following equation,

$$E_C = \frac{\nu_F E_F}{6} \qquad \text{Equation 2.3}$$

to describe the elastic modulus of particles randomly oriented in three dimensions without matrix material [Gibson, 1994]. As shown in Figures 2.7 and 2.8, this equation does not agree with the Christensen-Waals model as well as a relatively simple modified Cox model expressed by Tibbetts and McHugh:

$$E_C = (1-\nu_F)E_M + \psi\left[1-\frac{\tanh\beta}{\beta}\right]\nu_F E_F \qquad \text{Equation 2.4}$$

where β is:

$$\beta = {}^{\mathrm{L}}\!/_{\mathrm{d}}\sqrt{\frac{E_M}{(1+\nu)E_F \times \ln(\pi/4\nu_F)}} \qquad \text{Equation 2.5}$$

This model assembles Equations 2.1 and 2.3 and a model developed by Cox to predict the stresses along the length of a discontinuous fiber (particle) in a composite in tension [Johnson and Birt, 1991]. The coefficient β, defined by Equation 2.5, accounts for particle discontinuity and is a function of fiber aspect ratio, ${}^{\mathrm{L}}\!/_{\mathrm{d}}$, and matrix Poisson's ratio, ν. The coefficient ψ accounts for particle orientation and is set equal to 1 for aligned fibers and ${}^{1}\!/_{6}$ for three dimensionally random particles [Tibbetts and McHugh, 1999]. Christensen and Waals [1972] advise that it is physically impossible to produce a

composite with three dimensionally random particle orientation at high volume fractions. They suggest $v_F = 0.2$ as an upper bound for the application of models describing the three dimensionally random case.

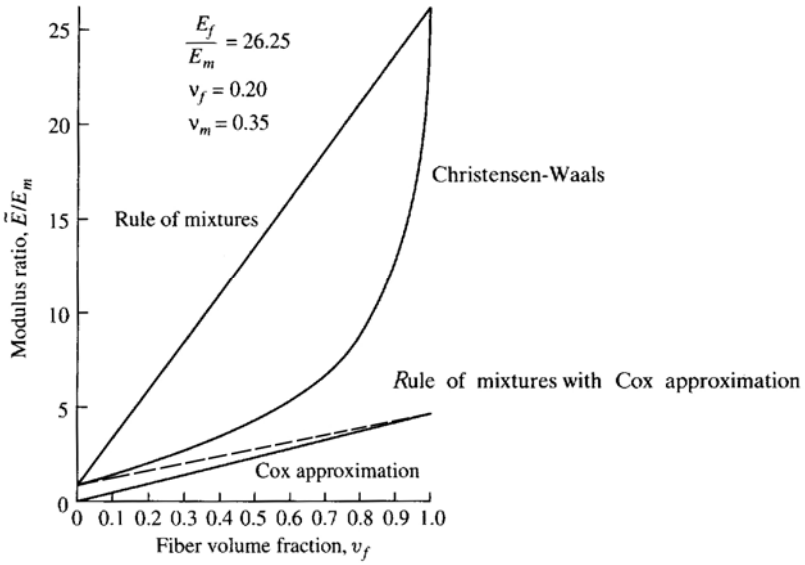

Figure 2.7 Comparison of Equation 2.1 (Rule of mixtures), the Christensen-Waals model, Equation 2.4 with $(\tanh\beta)/\beta = 0$ (Rule of mixtures with Cox approximation), and Equation 2.3 (Cox approximation) for a three dimensionally random case [Christensen and Waals, 1972].

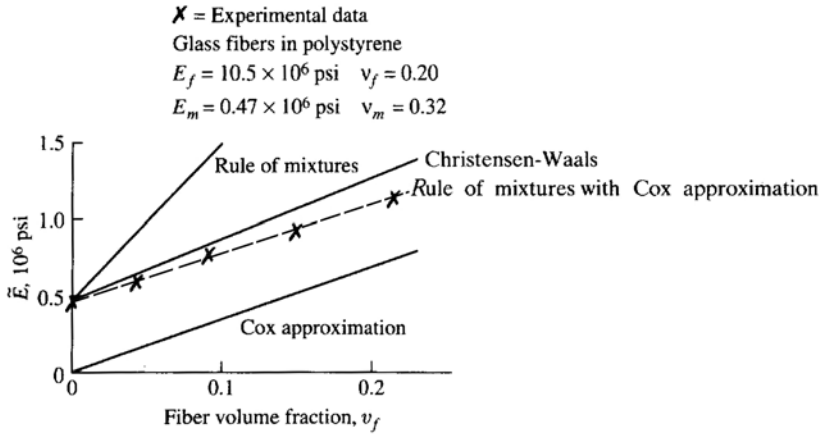

Figure 2.8 Comparison of experimental data with Equation 2.1 (Rule of mixtures), the Christensen-Waals model, Equation 2.4 with $(\tanh\beta)/\beta = 0$ (Rule of mixtures with Cox approximation), and Equation 2.3 (Cox approximation) for a two dimensionally random case [Christensen and Waals, 1972].

Figure 2.9 shows the potential influence of L/d on E_C. Barone and Schmidt [2005] measured E_C for polyethylene matrix composites containing 20 wt% chicken feather fibers with various L/d. Fibers of constant diameter (5 μm), obtained from Featherfiber Corporation, were ground using a centrifugal grinder or ball mill and then sieved on a vibratory mill to obtain fibers with lengths of 0.05, 0.2, 1, and 2 mm. Figure 2.9 shows that for fibers with an aspect ratio below a critical value, $(L/d)_c$, E_C is negatively influenced by the aspect ratio of the fibers. For fibers with aspect ratios above $(L/d)_c$, E_C is constant. Barone and Schmidt identified an $(L/d)_c$ of 50 for polyethylene matrix composites containing 20 wt% chicken feather fibers.

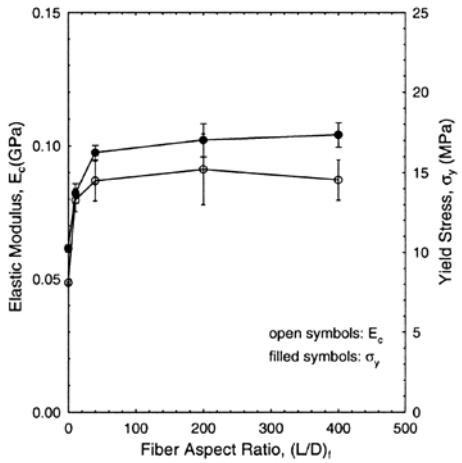

Figure 2.9 Composite elastic modulus and yield stress versus fiber aspect ratio, showing a critical aspect ratio of approximately 50 [Barone and Schmidt, 2005].

Tibbetts and McHugh [1999] used Equation 2.4 to predict the composite elastic modulus of vapor-grown carbon fiber (VGCF) polymer matrix composites. Theoretical values were compared with experimental results (Figure 2.10). Dumbbell tensile

specimens (ASTM D638 Type V) using VGCF/nylon and VGCF/polypropylene were injection molded after rotary mixing of the fibers and polymer melt. Experimental results were found to exceed theoretical values for three dimensionally random fibers, and it was concluded that injection molding oriented the fibers somewhat. Experimental values agreed, instead, with theoretical values for two dimensionally random fibers. The specimen fiber orientation was not studied [Tibbetts and McHugh, 1999]. According to Folkes [1982], an injection molded dumbbell specimen possesses predominant fiber orientation along the axis of the specimen (Figure 2.11). In fact, it is fiber alignment which has made these specimens popular for obtaining an upper bound for the tensile modulus of a composite.

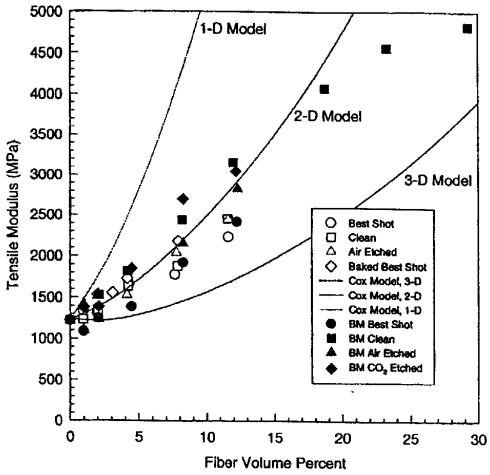

Figure 2.10 Young's modulus of VGCF/polypropylene composites as compared with Equation 2.4 [Tibbetts and McHugh, 1999].

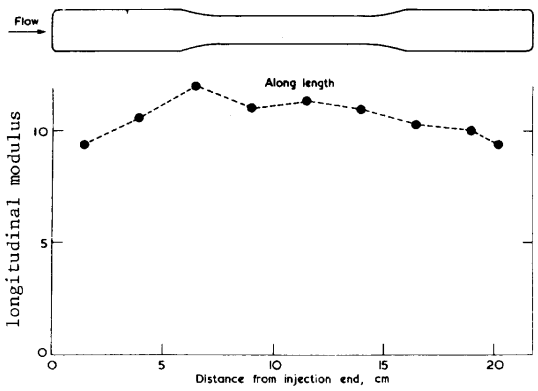

Figure 2.11 Elastic modulus as a function of distance from injection, showing that injection molding causes particle alignment to occur between the specimen ends [Folkes, 1982].

Paul [1960] proposed a model which describes the elastic modulus of a composite with cube-shaped inclusions. Paul's equation can be written in terms of inclusion modulus, E_F, inclusion volume fraction, v_F, and E_M:

$$E_C = \frac{E_M\left(E_M + \left(E_F - E_M\right)v_F^{\,2/3}\right)}{E_M + \left(E_F - E_M\right)v_F^{\,2/3}\left(1 - v_F^{\,1/3}\right)} \qquad \text{Equation 2.6}$$

Developed as a simple strength of materials approximation, it assumes strain compatibility among the constituents and that the constituents have identical Poisson's ratios. Paul's equation is neither a function of particle length nor orientation due to its assumption of cubic inclusions. It would equally apply to composites with aligned or randomly oriented inclusions [Johnson and Birt, 1991]. Figure 2.12 compares Equation 2.6, the Paul model, to Equation 2.1, the rule of mixtures. Given the same constituents, Equation 2.6 predicts a lower E_C than Equation 2.1, because Equation 2.6 accounts for the reduced contribution to E_C of particles with low aspect ratios (Figure 2.12a). Thus, for a given value of E_C, a rearranged Equation 2.6 predicts a higher value of E_F than a rearranged Equation 2.1 (Figure 2.12b).

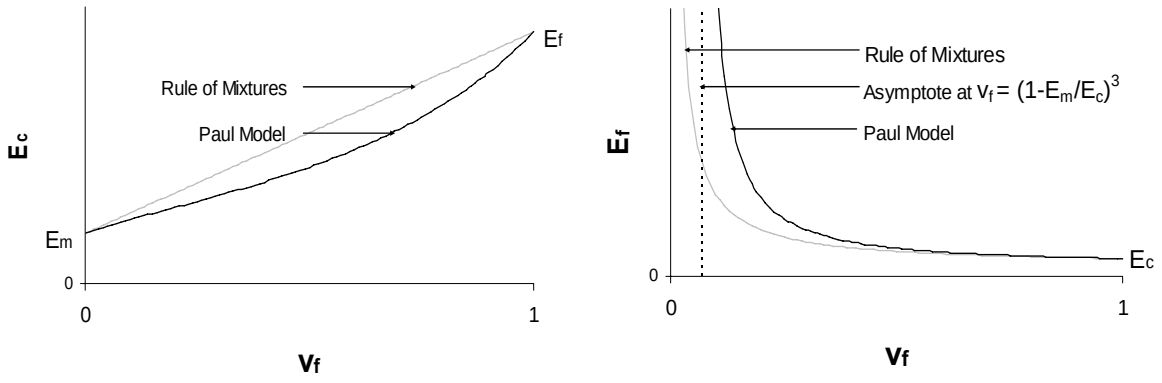

(a) (b)

Figure 2.12 (a) Comparison of Equation 2.1, the rule of mixtures, and Equation 2.6, the Paul model. (b) When expressed as a function of E_C, v_F, and E_M, the Paul's model behaves asymptotically.

Johnson and Birt [1991] examined the Cox model, Equation 2.4 with an assumption of aligned fibers (ψ=1), and the Paul model and compared their predictions with experimental results for SiCp particulate-reinforced aluminum matrix composites. The dimensions of the particles were typically less than 1 μm, and the aspect ratio of the particles was in the range of 1-2. The Cox model assumes that stresses are transferred to the particles through shear. Johnson and Birt suggest that at such a low aspect ratio, stresses cannot be transferred to the particles through shear, but instead must be introduced through the ends of the particles. This explains the low prediction by the Cox model for E_C, shown in Figure 2.13. While the Cox model under-predicts experimental results, the Paul model gives a good upper bound prediction for E_C. The Paul model may predict high values for E_C due to its assumption of cubic inclusions, which would have an aspect ratio of exactly 1. The reported Poisson's ratios of the matrix material and the particles were 0.32 and 0.17, respectively. This mismatch violates an assumption of

the Paul model and may have also affected agreement between the Paul model and experimental results.

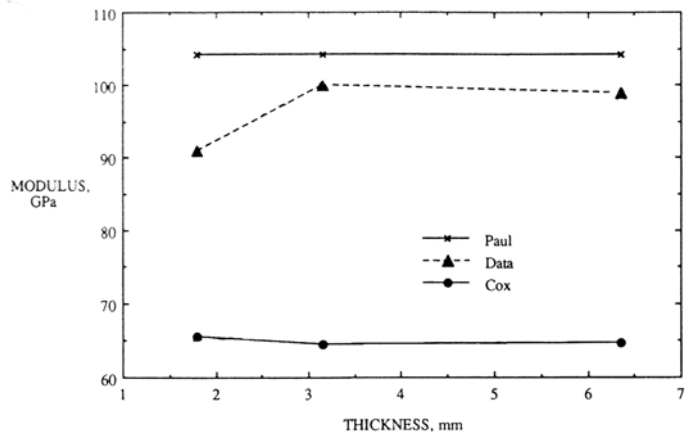

Figure 2.13 Comparison of theoretical values for E_C and experimental results for a particulate-reinforced composite, showing the Paul model as an upper bound prediction [Johnson and Birt, 1991].

The models presented are relevant to the determination of the Young's moduli of processed chicken feather fractions from composites with these particles randomly oriented in three dimensions. Though Equation 2.1 (a rule of mixtures) was developed for unidirectional continuous fiber composites, it can be applied to three-dimensionally random discontinuous fiber (particle) composites given an assumption of strain compatibility in the particles and matrix. Given this assumption, it can be used to determine the Young's modulus of the particle array, acting in bulk, without accounting for particle length or orientation. Equation 2.4 (a modified Cox Model) can be used to account for particle length and orientation due to its use of the variables β and ψ. Thus, Equation 2.4 can be used to determine the average particle longitudinal Young's modulus. As demonstrated by Johnson and Birt [1991], this equation is only applicable to particles with appreciable aspect ratios. Equation 2.6 can be applied to particles with aspect ratios approaching 1. While Equation 2.6 (the Paul model) is not applicable to

process chicken feather fiber, some processing regimes may produce quill particles with aspect ratios approaching 1.

2.3.3.2 Tensile Strength Analytical Models

Simple models readily describe the tensile strength of unidirectional continuous fiber composites, whereas more sophisticated models must be employed to describe randomly oriented short fiber (particle) composites.

A rule of mixtures similar to Equation 2.1 relates composite tensile strength (σ_C), matrix stress at the strain corresponding to particle tensile failure (σ_{M*}), and longitudinal particle tensile strength (σ_F):

$$\sigma_C = (1 - v_F)\sigma_{M*} + v_F \sigma_F \qquad \text{Equation 2.7}$$

This equation assumes that the composite fails at the particle tensile failure strain and that this value is less than the matrix tensile failure strain. This equation was developed for unidirectional continuous fiber composites from an assumption of strain compatibility [Gibson, 1994].

Composite failure can be caused by a number of mechanisms. In addition to particle failure, matrix failure and particle-matrix interface failure can contribute. The Tsai-Hill equation,

$$\sigma(\theta) = \left[\frac{\cos^4 \theta}{\sigma_L^2} + \left[\frac{1}{\tau^2} - \frac{1}{\sigma_L^2} \right] \sin^2 \theta \cos^2 \theta + \frac{\sin^4 \theta}{\sigma_T^2} \right]^{-1/2} \qquad \text{Equation 2.8}$$

describes the tensile strength, $\sigma(\theta)$, of an aligned continuous fiber composite as a function of the angle, θ, between the fibers and the direction of the applied load. It

assembles σ_L, the strength of the longitudinally loaded composite, σ_T, the transverse strength of the composite, and τ, the composite's shear strength.

Equations for σ_L, presented by Kelly and Tyson [1965], accommodate discontinuous fiber (particle) composites and take advantage of the concept of critical particle length, L_c. It is assumed that load is transferred into a particle by interfacial shear at the particle-matrix interface, that the matrix material is rigid-plastic, and that the shear strength of the particle-matrix interface, τ_i, is equal to matrix yield strength in shear. The critical particle length is the length required for shear stresses to transfer sufficient tensile stress to the particle such that it fractures. A particle shorter than this length will carry less stress than would a longer particle [Gibson, 1994]. For a set of particles with various diameters, it is useful to instead consider $\left(L/d\right)_c$, which is defined as follows:

$$\left(L/d\right)_c = \frac{\sigma_F}{2\tau_i} \qquad \text{Equation 2.9}$$

In terms of particle aspect ratio, L/d, σ_L can be expressed as:

$$\sigma_L = (1-v_F)\sigma_{M^*} + v_F\sigma_F\left[1 - \frac{\sigma_F}{4\tau_i\left(L/d\right)}\right] \qquad \text{for } \left(L/d\right) \geq \left(L/d\right)_c \qquad \text{Equation 2.10}$$

or

$$\sigma_L = (1-v_F)\sigma_{M^*} + v_F\tau_i\left(L/d\right) \qquad \text{for } \left(L/d\right) \leq \left(L/d\right)_c \qquad \text{Equation 2.11}$$

Figure 2.9 shows the potential influence of L/d on σ_C. Barone and Schmidt [2005] measured yield stress, defined as peak stress and here denoted σ_C, in addition to E_C, for polyethylene matrix composites containing 20 wt% chicken feather fibers with

various L/d. Figure 2.9 shows that for fibers with an aspect ratio below $(L/d)_c$, σ_C is negatively influenced by the aspect ratio of the fibers, just as is E_C. For fibers with aspect ratios above $(L/d)_c$, σ_C is constant. As it relates to both elastic modulus and tensile strength, Barone and Schmidt identified an $(L/d)_c$ of 50 for polyethylene matrix composites containing 20 wt% chicken feather fibers. Equation 2.9 shows that $(L/d)_c$ is dependent on both particle and particle-matrix interface properties. Thus, a different value of $(L/d)_c$ would likely be measured for composites containing the same chicken feather fibers in a different matrix material.

Baxter [1998] proposed a model which averages $\sigma(\theta)$ over three dimensions in order to describe the tensile strength of a randomly oriented short fiber (particle) composite. For the three-dimensionally random system:

$$\sigma_C = \int_0^{\pi/2} \sigma(\theta) \sin\theta d\theta \qquad \text{Equation 2.12}$$

This equation assumes that particle-interface failure occurs at a stress greater than the tensile strength of the matrix. Baxter defines σ_L with Equation 2.10 or 2.11. As simplifying assumptions, Baxter proposes that σ_T be set equal to the tensile strength of the matrix, σ_M, and that τ_i be set equal to τ. Baxter compared theoretical values to previously reported experimental data for three-dimensionally random particle-reinforced metal matrix composites. This model showed good agreement with results from Jones and Wawner [1989], Das *et al*. [1988], and Morimoto *et al*. [1987].

Tibbetts and McHugh [1999] used the Baxter model to predict the composite tensile strength, σ_C, of VGCF polymer matrix composites. As additional simplifying assumptions, τ and τ_i were set equal to $\frac{\sigma_M}{\sqrt{3}}$. This, in effect, sets σ_C equal to σ_M at $v_F = 0$. While E_C was successfully predicted with an assumption of two-dimensional randomness, experimental results exceeded Baxter model predictions for both two- and three-dimensionally random cases, as shown in Figure 2.14a. The authors suggest that a small ratio of VGCF length to L_c caused the theoretical results predicted by the Baxter model to be small. Thus, small ratios of particle length to L_c, or L/d to $\left(L/d\right)_c$, may cause the Baxter model to under-predict σ_C. For the VGCF, the ratio of L/d to $\left(L/d\right)_c$ was approximately $1/5$, given L/d=19.1. Alternatively, the ratio of L/d to $\left(L/d\right)_c$ for chopped FP Al_3O_3 fibers used in a three-dimensionally random system by Jones and Wawner [1989] was between $1/1$ and $1/0.4$, given L/d=10. Baxter's model successfully predicts these experimental results (Figure 2.14b).

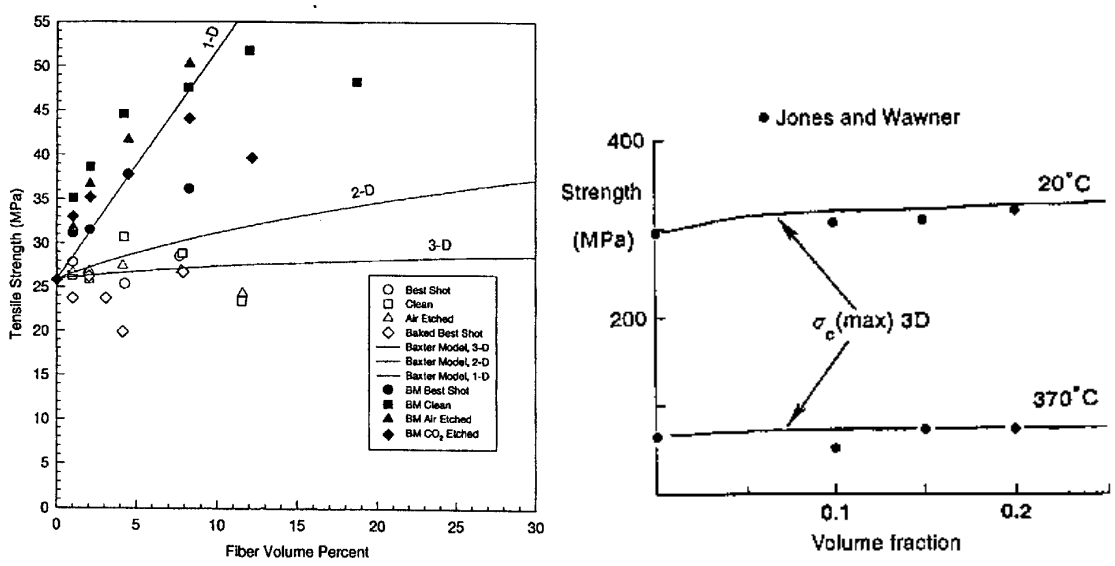

(a) (b)

Figure 2.14 Comparison between Equation 2.12 (Baxter Model, 3-D) and (a) experimental data for VGCF/polypropylene composites and (b) FP Al_2O_3/332 aluminum composites [Tibbetts and McHugh, 1999; Baxter, 1998; Jones and Wawner, 1989].

The models presented are relevant to the determination of the tensile strength of processed chicken feather fractions from composites with these particles randomly oriented in three dimensions. Though Equation 2.7 (a rule of mixtures) was developed for unidirectional continuous fiber composites, it can be applied to three-dimensionally random discontinuous fiber (particle) composites given an assumption of strain compatibility in the particles and matrix. Given this assumption, it can be used to determine the tensile strength of the particle array, acting in bulk, without accounting for particle length or orientation. Equation 2.12 can be used to account for particle length and orientation because it incorporates L/d and averages $\sigma(\theta)$ over three dimensions. Thus, Equation 2.12 can be used to determine the average particle longitudinal tensile

strength. However, Equation 2.12 may only be applicable to composites containing particles with $L/d \geq \left(L/d\right)_c$.

2.4 Summary

The existing literature includes physical, mechanical, and chemical durability data for keratin, and in some cases, chicken feather fractions. However, a comprehensive accumulation of data specifically for processed chicken feather fiber and quill is not available. The properties of feather fiber are expected to differ from those of quill. The moisture content of CFM is expected to be approximately 12%. However, it is expected to vary significantly in response to relative humidity. Apparent specific gravity values are expected to be approximately 0.8 or greater. Chemical durability results are expected to show that alkaline environments are more deleterious than acidic environments. Fiber length is expected to be approximately 3-13 mm, though different processing regimes likely produce different fiber lengths. Fiber diameter is expected to be approximately 5-50 μm. Fiber aspect ratio is expected to be approximately 400-2600. Young's modulus values are expected to be approximately 1-4 GPa. Tensile strength values are expected to be approximately 100-200 MPa. Mechanical property results will be affected by unexpected particle orientation.

CHAPTER III

EXPERIMENTAL PROCEDURES

3.1 Materials

All experiments examined samples of either processed chicken feather fiber or quill. Samples were either obtained directly from Tyson or MaXim LLC or processed from feathers collected at the Gold Kist chicken processing facility in Carrollton, Georgia, in May of 2004 and March of 2005.

Feathers collected at the Gold Kist chicken processing facility had been removed from chickens by hot water and mechanically driven rubber fingers and then diverted from the plant in a trough of water. The feathers were collected by hand from a conveyor belt carrying waste – chicken heads, feet, and feathers – to an offal truck. The feathers were transported on ice and then frozen, because feather masses which are commingled with chicken parts, water, and fats decompose in a biological process that is accelerated at high temperatures. The feathers were later cleaned in a washing machine with approximately 7 L of anti-microbial soap per m^3 of feathers and then dried in a rotary drier.

Table 3.1 shows the source of feathers and processing information. Processing involves grinding the feathers and separating them into fiber and quill fractions. All examined quill fractions were composed of both inner and outer quill. Details on how the feathers are processed are generally difficult to ascertain, as many of the processing techniques are proprietary. Sample B was cut by hand at Georgia Tech into fiber and quill fractions. The fiber fraction was then chopped with a household coffee grinder until

each fiber was separated. The quill fraction was chopped with the same grinder until each particle was 25 mm or less in length.

Prior to experimentation or oven-drying, all samples were conditioned in an environmental chamber at 23°C and 50% relative humidity for at least 3 weeks. Each oven-dried sample was dried at 110°C$\pm$5^{o} until its change in weight, weighed to the nearest 0.1 mg, during 24 hr of oven-drying was less than 0.5% of its weight before oven-drying (300 to 700 mg). 110°C is the experimentally-determined moisture evolution temperature of chicken feather fractions [Kock *et al*., 2005].

Table 3.1 Description of samples examined.

Sample	Feather Source	Processing
A	Gold Kist March 2005	MaXim LLC
B	Gold Kist May 2004	Manual
C		Tyson
D		MaXim LLC

For the Young's modulus and tensile strength tests, coupons were cut from cast polymer matrix composites containing Sample A fiber, oven-dried fiber, quill, or oven-dried quill. A two-component polyether-based urethane casting system was used as the matrix material. Forsch Polymer 80A Liquid, which produces a Shore 80A elastomer, was selected. Only previously unopened containers were used, to prevent moisture uptake by the urethane. For each casting, known masses of the base component and sample at a volume fraction of 0.00, 0.02, 0.04, or 0.08 were mixed and degassed for 5 min at 64 cm Hg while being vibrated. The mixture was heated to 34^{o}C and then mixed for 2 min with a mass of the activator component equal to 50% of the base component mass. This mixture was degassed for 10 min at 64 cm Hg while being vibrated. The mixture was then poured onto a rigid glass plate and covered with a rigid acrylic plate

separated from the first by glass or polyethylene spacers, as shown in Figure 3.1a. Each plate was twice spray coated with mold release (Universal Mold Release manufactured by Smooth-On) before use. The mixture cured, between rigid plates, for 2 days at room temperature ($22^{o}C \pm 1^{o}$) prior to cutting. Each casting yielded a 120-200 cm^3 sheet with a thickness of 5 mm, 10 mm, or 15 mm. To minimize discrepancies among individual coupons, coupons were cut radially from the center of each sheet, where the material was originally poured. Because the coupons were cut from poured sheets, three-dimensionally random fiber orientation is assumed. Injection molding would have caused fiber alignment along the axis of injection [Folkes, 1982].

(a) (b)

Figure 3.1 (a) Cast polymer composite sheets containing CFM during curing and (b) a cut coupon with a fiber volume fraction of 0.08.

3.2 Methods

Key physical properties, including moisture content, aspect ratio, apparent specific gravity, and chemical durability, were determined for processed fiber and quill. As well, key mechanical properties, including Young's modulus and tensile strength, were calculated for processed fiber and quill.

3.2.1 Physical Properties

3.2.1.1 Moisture Content

The moisture content of processed fiber and quill can vary depending upon processing and environmental conditions. An understanding of the moisture content of a particular sample is important for proportioning materials by mass, when a specific volume of the material itself (rather than the material and water) is needed.

The moisture contents of Sample A fiber and quill, Sample B fiber and quill, and Sample D fiber were measured. All samples were conditioned at 23°C and 50% relative humidity before an initial mass measurement was made to allow for consistency among different samples types. This initial mass is denoted W_{cond}. 300 to 700 mg of sample was used for each moisture content measurement. Samples were oven-dried at 110°C$\pm$5^{o} per the previous description. The final oven-dry weight (W_{od}) of each sample was recorded once its change in weight during 24 hours of oven-drying was less than 0.5% of the weight of the sample before oven-drying. The moisture content percentage was determined from:

$$MC = \frac{100(W_{cond} - W_{od})}{W_{od}} \qquad \text{Equation 3.1}$$

The moisture content was averaged for 4 replicate samples for each sample type.

3.2.1.2 Aspect Ratio

A particle's aspect ratio can affect its contribution to composite mechanical properties. The particle aspect ratio required for particle strength to fully be developed is proportional to particle diameter [Gibson, 1994]. Particle diameters, lengths, and aspect ratios were measured for Sample A fiber, oven-dried fiber, and quill. An optical

microscope (model MZ 6 manufactured by Leica) equipped with a digital camera (manufactured by Diagnostics Instruments, Inc.) was used to capture digital images. These images were used to measure particle length and diameter with image analysis software (Image-Pro Plus 4.5.1.). For each sample type, particles were sparsely dispersed on a glass precleaned microscope slide and covered with a plastic microscope cover slip, which was sealed in place with clear nail polish. For the slide containing fiber and the slide containing oven-dried fiber, images at two distinct locations were captured at both 50x magnification (zoomed in) and 25x magnification (zoomed out). For each slide location, the length and diameter of all particles contained within or touching a 1.75 by 2.25 mm frame were measured (Figure 3.2). For the slide containing quill, images at two distinct locations were captured at both 25x magnification (zoomed in) and 12.5x magnification (zoomed out). For each slide location, the length and diameter of all particles contained within or touching a 3.5 by 4.5 mm frame were measured. The dimensions of each particle found to be in focus and with a length greater than 0.1 mm was recorded. The zoomed in image was used for measuring particles within the frame, while the zoomed out image was used for measuring particles touching and extending out of the frame. Measurements to the nearest μm were made using optical analysis software, which was calibrated for each level of magnification utilized. Two lines, one longitudinal and one transverse, were drawn to the extents of each particle with the optical analysis software, which gave the dimension of each line. Segmented straight lines were traced over curved particles in order to determine the longitudinal dimension of such particles.

For each particle, the aspect ratio was calculated as the length divided by the diameter. Length, diameter, and aspect ratio were averaged for a minimum of 60 particles for each sample type.

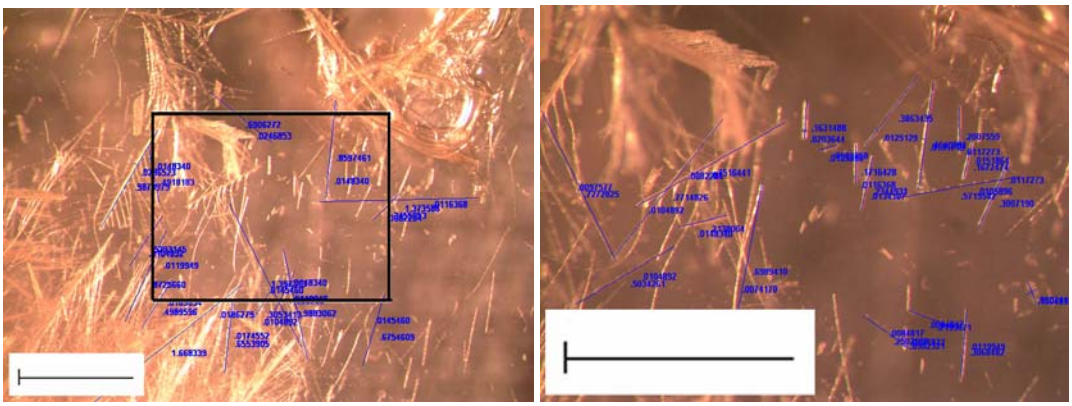

(a) (b)

Figure 3.2 (a) Image of oven-dried fiber at 25x magnification used to determine the dimensions of particles touching and extending out of a 1.75 by 2.25 mm frame and (b) image of the same at 50x magnification used to determine the dimensions of particles within the frame. Scalebar length is 1 mm.

3.2.1.3 Apparent Specific Gravity

Many applications for CFM could be motivated by its low relative density. However, the densities of CFM have not been well-characterized in the literature. One measurement by Wool *et al*. [2004] for the density of chicken feather fiber was reported as 0.8 g/cm^3, while another by Barone and Schmidt [2005] was reported as 0.89 g/cm^3. In order to better understand the properties of fiber and quill fractions, as well as the variability among sources of CFM, the apparent specific gravities of fiber and quill fractions were measured (Table 3.2). These measurements were used to calculate the particle volume fractions of composites containing fiber and quill fractions which were used for mechanical property testing.

A gravimetric procedure similar to that described in ASTM C128-04a, "Standard Test Method for Density, Relative Density (Specific Gravity), and Absorption of Fine

Aggregate" was used to measure apparent specific gravity. The ASTM C128-04a procedure describes gravimetric and volumetric methods for measuring apparent specific gravity that involve submerging samples in water. To overcome the issue of feather wetability, 95% ethanol with a known density was used instead of water. Ethanol has been shown by Griffith [2002] to remove a fatty layer from the surface of feathers, and the removal of this layer, according to Negri [1993], can reduce the hydrophobic nature of feathers. Because of the tendency of samples to float, even in ethanol, a gravimetric method rather than a volumetric method was used. Table 3.2 shows that a minimum of 4 replicate runs were performed for each sample type except when sample availability was limited (as with Sample A oven-dried quill and Sample C fiber).

Table 3.2 Apparent specific gravity measurements performed.

Type	Vacuum (cm Hg)	Minimum Number of Measurements
A Fiber	36	10
A Fiber	0	4
A Fiber	67	4
A Oven-dried Fiber	36	4
A Quill	36	4
A Oven-dried Quill	36	2
B Fiber	36	4
B Oven-dried Fiber	36	4
B Quill	36	4
C Fiber	36	2

For each run, between 100 and 600 mg of sample was placed in ethanol in a pycnometer (Figure 3.3a) and degassed at 67 cm Hg, 36 cm Hg, or 0 cm Hg for 10 min. As in ASTM C128-04a, the apparent specific gravity of the sample was determined from:

$$SG_{apparent} = \frac{A}{(B + A - C)} \qquad \text{Equation 3.2}$$

where A is the mass of the sample (g), B is the mass of the pycnometer filled with ethanol to a calibrated volume (g), and C is the mass of the pycnometer filled with the sample and ethanol to a calibrated volume (g). The apparent specific gravity calculated by Equation 3.2 was multiplied by the specific gravity of the ethanol (i.e., 0.8159) to account for the use of ethanol in place of water. The apparent specific gravity was averaged for replicate samples.

This method was validated by making measurements of a solid material of known density in several solutions of known density. The specific gravity of polystyrene flakes was measured in ethanol, deionized water, and mineral oil. The average reading for the polystyrene flakes in each solution was found to be within 2% of the specific gravity reported by the manufacturer (i.e., 1.04), thus validating the methodology.

(a) (b)

Figure 3.3 (a) Pycnometer used for apparent specific gravity measurements and (b) degassing chamber.

3.2.1.4 Chemical Durability

The durability of Sample A fiber and quill was examined in mildly acidic, near-neutral, mildly alkaline, and strongly alkaline solutions to preliminarily assess potential incompatibilities between CFM and matrix materials and also environmental conditions

to which CFM-based composites might be exposed. In order to assess durability, mass loss of filtered, washed, and dried replicate samples over time was measured.

Previously oven-dried CFM samples (Table 3.3) were stored at room temperature ($22^{o}C \pm 1^{o}$) in solutions tailored to replicate conditions in cement-based, wood, and gypsum composites. For each measurement, 120 to 170 mg of oven-dried sample, weighed to the nearest 0.1 mg, was stored in 50 ml of solution. A concentrated sodium hydroxide solution (0.7M NaOH with pH=12.4) was selected to replicate conditions in a cementitious matrix [Gentry, 2001]. A saturated gypsum solution was used to model gypsum composite conditions. The molarity of the solution (0.014M with pH=7.7) was determined from the solubility limit of gypsum. A dilute acetic acid solution ($1.6e^{-8}$M $C_2H_4O_2$ with pH=6.0) was utilized to model wood composite conditions [Bootle, 1983]. The molarity of the solution was determined experimentally by combining acetic acid and deionized water until a solution pH of 6 was reached. The solutions, then, provided a range of pH conditions and replicated some potential conditions in composite materials.

Table 3.3 Chemical durability measurements performed.

Type	Solution	Duration	Minimum Number of Measurements
Fiber, Quill	Water	0	6
Fiber, Quill	Water	7	3
Fiber, Quill	Acetic	7	3
Fiber, Quill	Gypsum	7	3
Fiber, Quill	NaOH	7	3
Fiber, Quill	Water	28	3
Fiber, Quill	Acetic	28	3
Fiber, Quill	Gypsum	28	3
Fiber, Quill	Water	56	3
Fiber, Quill	Acetic	56	3
Fiber, Quill	Gypsum	56	3
Fiber, Quill	Water	90	3
Fiber, Quill	Acetic	90	3
Fiber, Quill	Gypsum	90	3
Fiber, Quill	Water	120	3
Fiber, Quill	Acetic	120	3
Fiber, Quill	Gypsum	120	3

At 0, 7, 28, 56, 90, and 120 days, designated samples were filtered, washed with deionized water, filtered, oven-dried at 110°C$\pm$5^{o} per the previous description, and then weighed. 0.45 μm pore size filters (manufactured by Millipore with hydrophobic edge membranes) in a reusable filter holder (Figure 3.4b) attached to a Venturi vacuum pump were used for filtration. Percent mass loss was calculated for each sample and averaged for 3 replicate samples. Samples soaked in deionized water (with a resistivity of 18.2 MΩ) were used as control samples.

(a) (b)

Figure 3.4 (a) Vials of CFM in mildly acidic, near-neutral, mildly alkaline, and strongly alkaline solutions and (b) the device used for filtration.

3.2.2 Mechanical Properties

The development of successful applications for CFM will be aided by an understanding of their mechanical properties. Selecting compatible matrix materials for CFM will specifically require an understanding of the Young's moduli of chicken feather fractions. While studies have been executed which document some mechanical properties of individual chicken feather fibers [Hong and Wool, 2005] and whole ostrich feather rachis [Taylor *et al.*, 2004], changes that might occur during processing and the heterogeneity of processed chicken feather fractions suggest that these results may not adequately represent the properties of processed fractions. This motivates a separate and comprehensive study of processed fiber and quill.

Young's modulus and tensile strength were measured for replicate polymer matrix composite coupons containing CFM. Table 3.4 specifies the coupon types and minimum number of replicates tested. Particle volume fractions (v_F) of 0.08 or less were selected because degassing failed to adequately remove air voids at higher values of v_F. Straight-sided coupons with nominal dimensions of 114 x 21 mm were selected. Coupons were tested in uniaxial tension at a rate of 5 mm/min, in accordance with ASTM D638-03,

"Standard Test Method for Tensile Properties of Plastics." Load and strain were recorded to the nearest 0.000001 lb and 0.0001% strain using LabVIEW 5.1.1 software. Load was measured with a 1000-lb load cell calibrated for 0-50 lb measurements. Strain was measured with a 1-in gage length extensometer calibrated for 0-0.25% strain measurements.

Table 3.4 Composite coupons tested.

Type	vf	Thickness (mm)	Minimum Number of Coupons
Neat	0.00	5	18
Fiber	0.02	5	12
Fiber	0.04	5	12
Fiber	0.08	5	12
Oven-dried Fiber	0.02	5	6
Oven-dried Fiber	0.04	5	6
Oven-dried Fiber	0.08	5	6
Quill	0.04	5	6
Oven-dried Quill	0.04	5	6
Fiber	0.04	10	6
Fiber	0.04	15	6

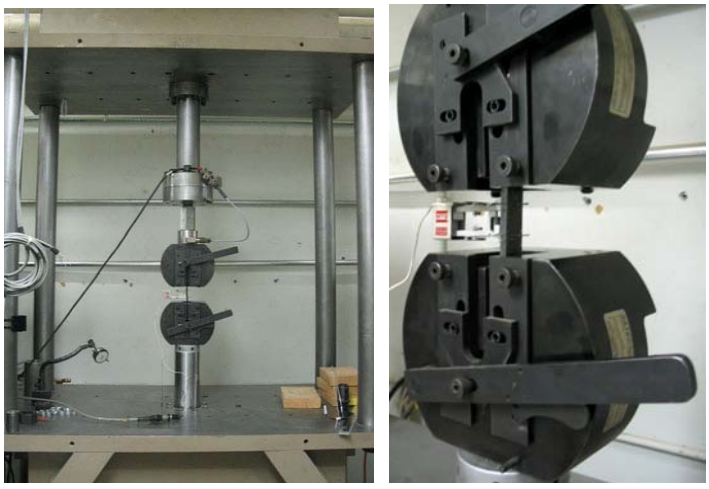

Figure 3.5 The test frame used for mechanical testing of coupons.

3.2.2a Young's Modulus

The Young's modulus of each coupon was calculated according to ASTM E111-04 at strains equal to or less than 0.25%. This value was selected because modulus

determinations made at strains in excess of 0.25% strain require the use of instantaneous properties (cross section and gage length).

Composite Young's modulus, E_C, was determined from the average Young's modulus for each set of replicate coupons. The Young's modulus of the matrix material, E_M, was set equal to the average Young's modulus of the neat coupons (v_F=0). For each set of replicate coupons, E_C and E_M were used to calculate effective particle Young's modulus, $E_{F-Effective}$, and particle Young's modulus, E_F, which represents the longitudinal Young's modulus of a single particle. $E_{F-Effective}$ represents the contribution to composite Young's modulus of the included particles, which is the Young's modulus of the particles when considered as a three-dimensional array with a particular orientation and aspect ratio distribution. If and only if the particles are aligned continuous fibers, E_F is equal to $E_{F-Effective}$. $E_{F-Effective}$ is introduced in order to allow simplified comparisons among samples. While calculation of E_F requires characterization of sample orientation and aspect ratio, calculation of $E_{F-Effective}$ does not.

For each sample type at each v_F, $E_{F-Effective}$ was calculated from the following rule of mixtures equation, which is Equation 2.1 expressed in terms of $E_{F-Effective}$:

$$E_{F-Effective} = \frac{E_C - (1 - v_F)E_M}{v_F} \qquad \text{Equation 3.3}$$

For each set of replicate coupons, E_F was calculated using a modified Cox Model, expressed by Equations 2.4 and 2.5, which can be solved iteratively for E_F. The coefficient β, defined by Equation 2.5, is incorporated to account for particle aspect

ratio, L/d. Because of the heterogeneous nature of processed fiber and quill fractions, the average L/d of each fraction was utilized, as opposed to the average length divided by the average diameter for each fraction. The model also incorporates the coefficient ψ to account for random particle orientation. ψ was set equal to $1/6$ in accordance with an assumption of three-dimensionally random particle orientation. The matrix Poisson's ratio, ν, was set equal to 0.5, the value reported by the manufacturer. The average E_C for each set of replicate coupons was compared with curves calculated using Equations 2.1 and 2.3.

For quill and oven-dried quill, particle Young's modulus was calculated using Paul's model, which can be expressed as:

$$E_{F-Effective} = E_F = \frac{E_M\left(E_M - E_C\right)}{E_C {\nu_F}^{2/3}\left(1 - {\nu_F}^{1/3}\right) - E_M {\nu_F}^{2/3}} \qquad \text{Equation 3.4}$$

3.2.2b Tensile Strength

The maximum stress value for each composite coupon was recorded as its tensile strength, σ_C. For each coupon that experienced particle fracture at failure, σ_C was used to calculate its effective tensile strength, $\sigma_{F-Effective}$, and its particle tensile strength, σ_F, which represents the longitudinal tensile strength of a single particle. $\sigma_{F-Effective}$ represents the contribution to composite tensile strength of the included particles, which is the tensile strength of the particles when considered as a three-dimensional array with a particular orientation and aspect ratio distribution. If and only if the particles are aligned continuous fibers, σ_F is equal to $\sigma_{F-Effective}$. $\sigma_{F-Effective}$ is introduced in order to allow

simplified comparisons among samples. While calculation of σ_F requires characterization of sample orientation (Equation 2.12 assumes a three-dimensionally random system) and aspect ratio, calculation of $E_{F-Effective}$ does not.

The fracture surface of each coupon was visually evaluated, and coupons were sorted into two groups, those which experienced particle pull-out at failure and those which experienced particle fracture at failure. The presence of exposed particles extending beyond the matrix material at the fracture surface was considered evidence of particle pull-out. Coupons with fracture surfaces lacking such exposed particles were considered to have experienced particle fracture at failure.

For each coupon that experienced particle fracture at failure, $\sigma_{F-Effective}$ was calculated from the following rule of mixtures equation, which is Equation 2.7 expressed in terms of $\sigma_{F-Effective}$:

$$\sigma_{F-Effective} = \frac{\sigma_C - (1-v_F)\sigma_{M*}}{v_F} \qquad \text{Equation 3.5}$$

For each coupon that experienced particle fracture at failure, the strain value corresponding to σ_C, ε_C, was used to calculate σ_{M*}, the stress in the matrix material at the maximum coupon stress value. From the stress-strain data for at least 6 neat coupons, the average matrix stress corresponding to ε_C was determined. σ_{M*} was set equal to this value for each composite coupon. Data from additional neat coupons was incorporated as needed until the coefficient of variation of σ_{M*} was $\leq$ 5% for each coupon. $\sigma_{F-Effective}$ was averaged for each set of replicate coupons. In addition, the average σ_C was calculated for each set of replicate coupons and compared with curves calculated using

Equation 2.7 and values of σ_{M*} equal to the average σ_{M*} for each set of replicate coupons.

For each sample type that experienced particle fracture at failure, σ_F was estimated using Baxter's model. Average σ_C values, calculated for each set of replicate coupons, were compared to curves calculated using Equation 2.12, which incorporates Equations 2.8 and 2.10. From Equation 2.8, the transverse strength of an equivalent aligned continuous fiber composite, σ_T, was set equal to the tensile strength of the matrix, σ_M, in accordance with simplifying assumptions proposed by Baxter [1998]. From Equations 2.8 and 2.10, the shear strength of an equivalent unidirectional continuous fiber composite, τ, and the shear strength of the fiber-matrix interface, τ_i, were set equal to $\frac{\sigma_M}{\sqrt{3}}$ in accordance with simplifying assumptions proposed by Tibbetts and McHugh [1999]. From Equation 2.10, L/d was set equal to the average L/d of each fraction. Values of σ_{M*} were set equal to the average σ_{M*} for each set of replicate coupons. Experimental data was first compared to curves with $\sigma_F = 2\tau_i\left(L/d\right)$. At this value of σ_F, Baxter's model predicts a maximum value of σ_C. At greater values of σ_F, L/d is less than the critical aspect ratio, $\left(L/d\right)_c$, which is a function of σ_F defined by Equation 2.9. When $L/d < \left(L/d\right)_c$, the Baxter's model prediction for σ_C is no longer a function of σ_F, because the particles fail to develop their full tensile strength. Thus, a composite containing particles with $L/d < \left(L/d\right)_c$ cannot be used to estimate σ_F. Experimental data was compared to curves calculated using Equation 2.12 and values of

$\sigma_F \leq 2\tau_i \left(L/d \right)$ in order to estimate a value of σ_F for each sample type that experienced particle fracture at failure.

CHAPTER IV

RESULTS AND DISCUSSION

4.1 Physical Properties

4.1.1 Moisture Content

Measurements of moisture content were made on Sample A and B fiber and quill and Sample D fiber after storage in a controlled temperature (23°C) and humidity (50% RH) environment. Averaged results for replicate samples are shown in Figure 4.1. The moisture contents of the samples were found to be between 16% and 20%. Moisture content was found to vary by sample. The moisture contents of fiber and quill fractions were found to be approximately the same.

The composition of chicken feathers has been reported as 91% protein (keratin), 1% lipid, and 8% water [Lederer]. Moisture contents of 16%-20% indicate that CFM are hygroscopic. This is supported by prior research by Yokota and Kunitake [2004]. The ability of CFM to absorb moisture from the environment has important implications for the processing, storage, transportation, and durability of CFM-containing composite materials, as increases in moisture content may interfere with processing or bonding, increase weight (and hence transportation costs), or lead to more rapid deterioration. Further research is required to determine the maximum suitable moisture content of CFM and also to assess the effect of variations in moisture on processing, storage, transportation, and durability.

As well, further research is required in order to determine the effect of oven-drying at various temperatures. It would be beneficial to reduce CFM weight by

minimizing moisture content prior to transportation, for example. However, oven-drying at 110°C±5°C was found to alter the color of CFM and thus potentially its structure or properties. Over the course of 1-4 weeks of oven-drying, the color of the CFM changed from white to a light, yellowish brown. DSC results indicate that temperatures below 110°C may not allow for the evolution of moisture [Kock *et al.*, 2005]. An optimal temperature for oven-drying CFM should be determined.

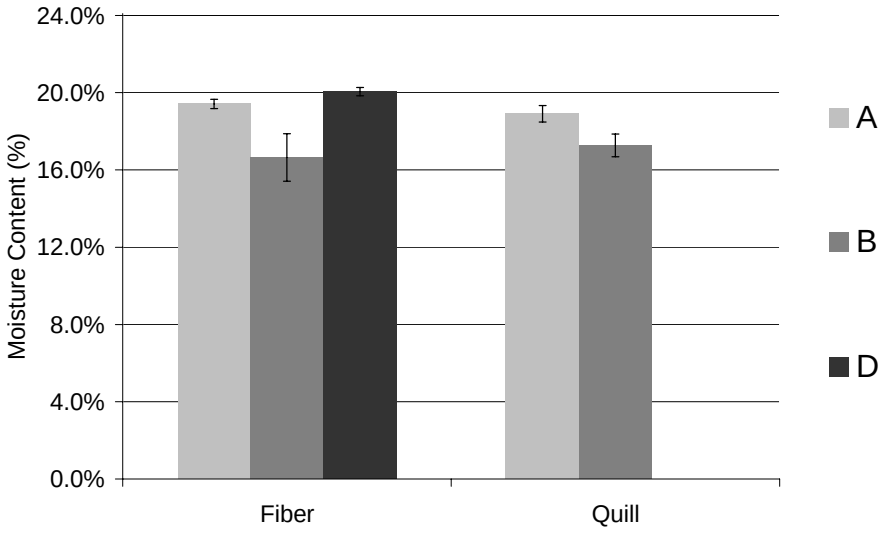

Figure 4.1 Moisture contents measured for Sample A and B fiber and quill and Sample D fiber after environmental conditioning.

4.1.2 Aspect Ratio

Length, diameter, and aspect ratio results for Sample A fiber, oven-dried fiber, and quill are shown in Figures 4.3, 4.4, and 4.5. These results are summarized, and the maximum measured length for each sample type is listed in Table 4.1. Average fiber and oven-dried fiber diameter was approximately 15 μm, while average quill diameter was approximately 120 μm. The coefficients of variation for the data were high due to the heterogeneity of each sample and the fact that the "fiber fraction" actually contains some

quill and vice versa. The coefficients of variation were approximately 120%, 80%, and 260% for fiber, oven-dried fiber, and quill, respectively. In order to evaluate segregated fiber and quill, a diameter value was selected for the purpose of delineating between fiber and quill. Figure 4.2 shows the percentage of fiber and oven-dried fiber diameters and the percentage of quill diameters that fall into each of nine diameter categories. Per Figure 4.2, a delineating diameter value of 30 μm was selected. While there are fibers and oven-dried fibers in every diameter category below the 31-35 μm category, no fibers or oven-dried fibers are in the 31-35 μm or 36-40 μm categories. Thus, it is assumed that 30 μm represents the upper boundary for fiber diameter.

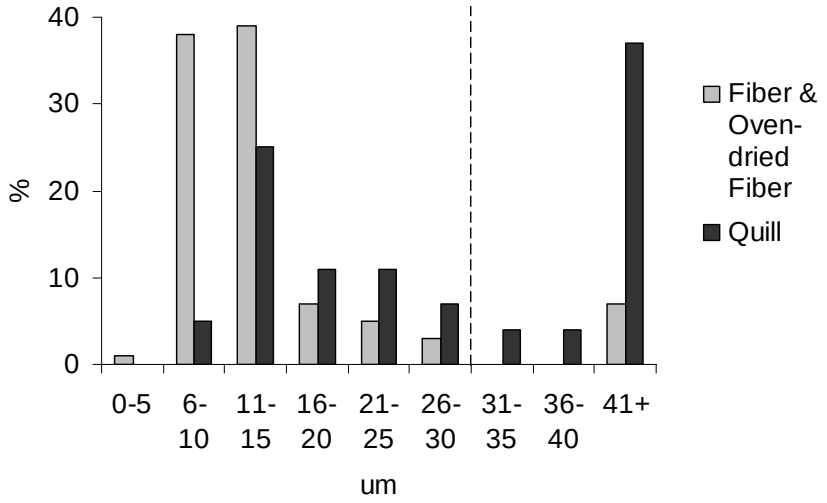

Figure 4.2. Percentage of fiber and oven-dried fiber diameters and the percentage of quill diameters that fall into each of nine diameter categories.

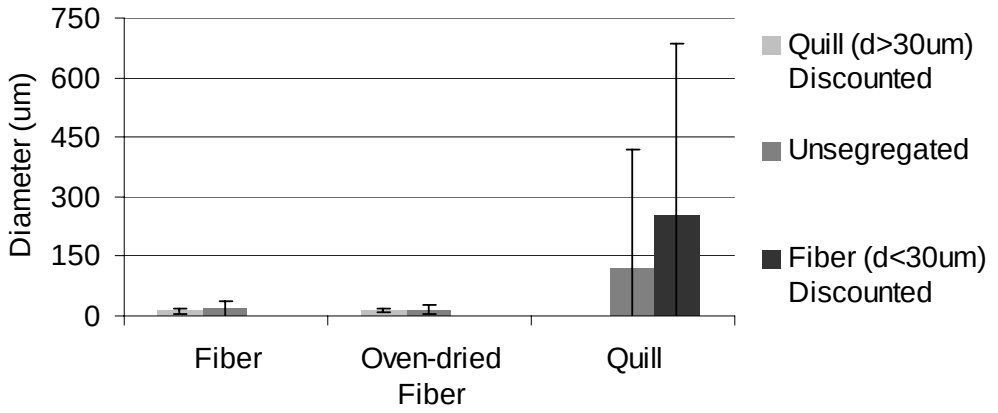

Figure 4.3. Diameters of segregated and unsegregated Sample A fiber, oven-dried fiber, and quill.

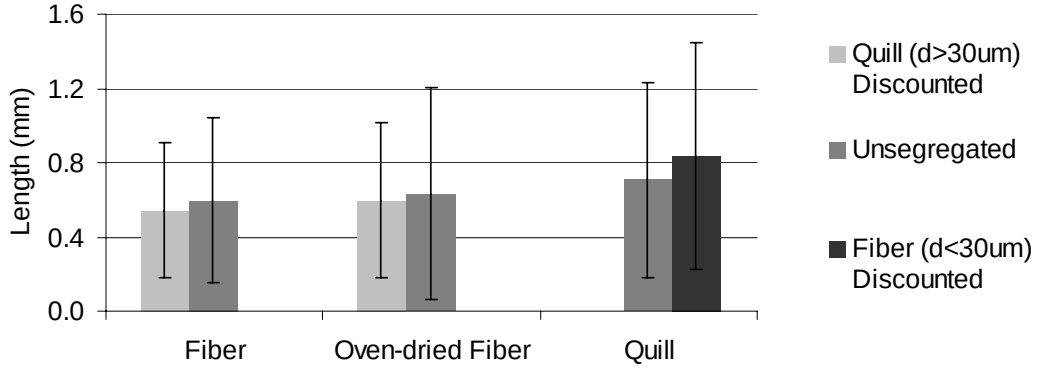

Figure 4.4. Lengths of segregated and unsegregated Sample A fiber, oven-dried fiber, and quill.

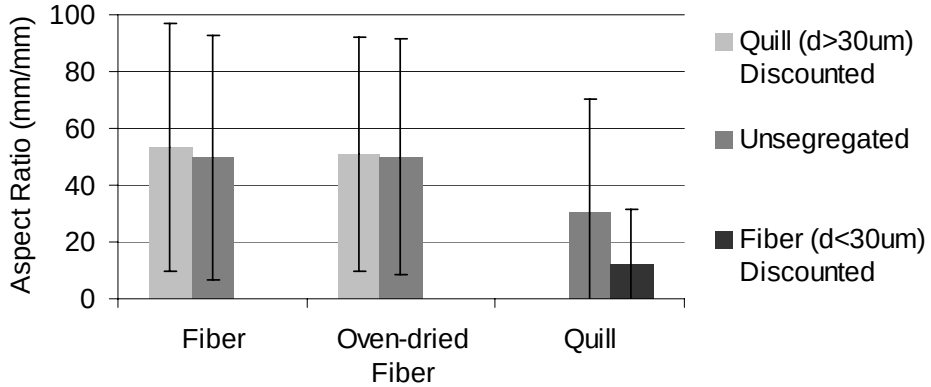

Figure 4.5. Aspect ratios of segregated and unsegregated Sample A fiber, oven-dried fiber, and quill.

Table 4.1. Lengths, diameters, aspect ratios, and maximum lengths of Sample A fiber, oven-dried fiber, and quill.

Type	Length (mm)	Diameter (um)	Aspect Ratio (mm/mm)	Maximum Length (mm)
Fiber	0.60 (0.44)	17 (20)	50	2.1
Oven-dried Fiber	0.63 (0.57)	15 (12)	50	3.6
Quill	0.71 (0.52)	118 (303)	31	2.7

After neglecting particles with diameters greater than 30 μm, the average fiber and oven-dried fiber diameters decreased. The coefficients of variation for fiber and oven-dried fiber decreased to approximately 40%, validating the assumption that 30 μm is a suitable upper bound for fiber diameter. After neglecting particles with diameters less than 30 μm, the coefficient of variation for quill decreased to approximately 170%, and the average quill diameter increased to approximately 250 μm, as shown in Figure 4.3.

Figure 4.4 shows that average fiber and oven-dried fiber length was approximately 0.6 mm, while average quill length was approximately 0.7 mm. After particles with diameters greater than 30 μm were neglected, the average fiber and oven-dried fiber length decreased slightly. Accordingly, after particles with diameters less than 30 μm were neglected, the average quill length increased to 0.8. This suggests that the quill particles are longer than the fibers, on average. After neglecting particles, coefficients of variation decreased slightly for fiber, oven-dried fiber, and quill. Maximum lengths for each of fiber, oven-dried fiber, and quill ranged from 2.1 to 3.6 mm.

Figure 4.5 shows that the average fiber and oven-dried fiber aspect ratio was 50, while the average quill aspect ratio was approximately 30. After particles with diameters greater than 30 μm were neglected, the average fiber and oven-dried fiber aspect ratio

increased slightly. After particles with diameters less than 30 μm were neglected, the average quill aspect ratio decreased by more than half to approximately 10. After neglecting particles, coefficients of variation decreased slightly for fiber and oven-dried fiber, and increased from approximately 130% to approximately 160% for quill. The aspect ratio of the fiber material is less variable than that of the quill material. Therefore, by neglecting particles with diameters less than 30 μm, the quill variability was increased.

All aspect ratio fractions studied were processed by MaXim LLC (Sample A). Fiber diameter results agree with those published by Kar and Misra [2004], who found the diameter of chicken down feather fibers obtained from MaXim LLC to be in the range of 5-50 μm. Values for the diameter of chicken feather fibers obtained from Featherfiber Corporation were reported by Dweib *et al*. [2004] and Barone and Schmidt [2005]. Values ranged from 3-13 μm. Hong and Wool [2005] reported a diameter value of 6 μm for chicken feather fiber obtained from Tyson Foods, Inc. Diameter results reported for fibers obtained from Featherfiber Corporation and Tyson Foods, Inc. are in better agreement with fiber and oven-dried fiber results after neglecting particles with diameters greater than 30 μm. Because the particles with diameters greater than 30 μm are considered to be quill particles, results indicate that fibers processed by MaXim LLC contain much more of the quill material than those processed by Featherfiber Corporation and Tyson Foods, Inc. This accounts for the wide diameter range reported by Kar and Misra [2004], as well. Lengths reported for fibers processed by Featherfiber Corporation were in the range of 3-13 mm [Dweib *et al*., 2004; Barone and Schmidt, 2005], while fibers processed by Tyson Foods, Inc. were reported to have typical lengths of 8 mm

[Hong and Wool, 2005]. A maximum length for fiber and oven-dried fiber of 3.6 mm suggests that processing by MaXim LLC produces significantly shorter fibers than processing by Featherfiber Corporation or Tyson Foods, Inc.

4.1.3 Apparent Specific Gravity

Apparent specific gravity results, measured on replicate samples of Samples A, B, and C, are shown in Figure 4.6. The data shows that apparent specific gravities ranged from approximately 0.7 to approximately 1.2. The apparent specific gravity of processed chicken feather fiber varied by source between 1.0 and 1.2. The quill, actually a mixture of inner and outer quill, was found to have an apparent specific gravity of between 0.7 and 0.9, which is less than that of the fiber.

The effect of oven-drying on specific gravity was also assessed, as oven-dried particles may be useful for composite production due to their well-defined moisture content. Values for oven-dried fiber were between 1.1 and 1.2, and the apparent specific gravity of oven-dried fiber was found to be greater than that of fiber conditioned at 50% RH for each fiber sample examined. Greater values for oven-dried fiber may be due to the loss of water, which has a specific gravity of 1, during oven-drying. Oven-dried quill was found to have approximately the same apparent specific gravity as quill.

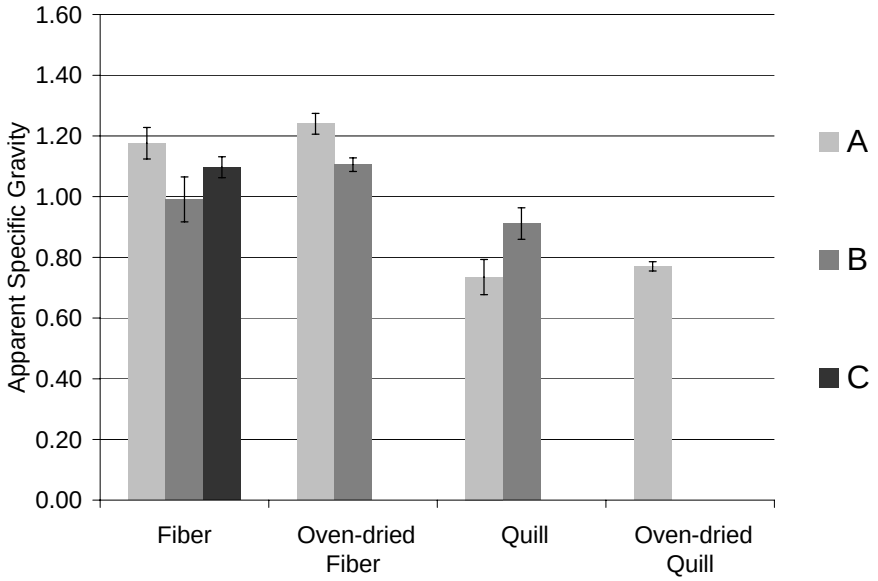

Figure 4.6 Apparent specific gravities of fiber, oven-dried fiber, quill, and oven-dried quill for Samples A, B, and D.

While the apparent specific gravities of Sample A fiber and quill were approximately 1.2 and 0.7, respectively, those of Sample B fiber and quill were approximately 1.0 and 0.9, respectively. Knowing that these materials were both collected from the same chicken processing plant, this suggests that Sample A's fractions are better segregated than those of Sample B. The apparent specific gravity of a fraction is likely influenced by the effectiveness of segregation during processing, and thus specific gravity measurements may be used to indicate the degree of segregation.

These values for fiber apparent specific gravity are greater than the density value of 0.8 g/cm^3 reported for chicken feather fiber by Hong and Wool [2005]. Such a difference may be due to variations in apparent specific gravity among samples from different sources. In addition to sample variation, different processing methods can affect the amount of the quill material included with the fiber material and vice versa. Alternatively, if Hong and Wool's [2005] value is falsely low, the results of their 2005

study, in which it was concluded that feather fiber soy resin matrix composites were created with a 5% filling of the hollow fibers with matrix material, might be better explained by unfilled fibers with an apparent specific gravity greater than 0.8.

Barone and Schmidt [2005] also compared density measurements of composites containing chicken feather fiber with predictions based upon constituent densities. A value for chicken feather fiber of 0.89 g/cm^3 was used to predict composite density. Feather fiber polyethylene matrix composites were found to have higher densities than predicted. A higher value for the apparent specific gravity of chicken feather fiber than 0.89 could potentially explain these results.

A value greater than 1.0 for the apparent specific gravity of fiber agrees with observations of the behavior of Sample A fractions in deionized water. The fiber fraction tends to sink, while the quill fraction tends to float. This tendency is depicted in Figure 4.7, which shows a tapered plastic cylinder containing Sample A fiber (which contains both fiber and quill particles) which has been drained of deionized water. The floating quill particles were deposited on the walls of the cylinder and thus separated from the sinking fibers. However, an alternative explanation is that water cannot infiltrate the porous inner quill, while it can infiltrate the hollow fibers. The contained air of the inner quill would thus cause it to float, while the fibers would likely sink, as the density of the solid matter of CFM is approximately 1.3 g/cm^3, the density of keratin [Arai *et al*., 1998].

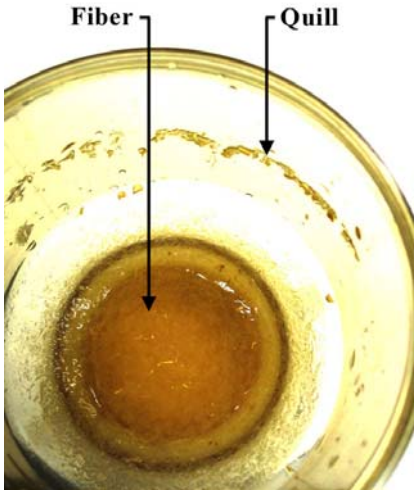

Figure 4.7 Separation of quill from fiber due the fact that the quill floated and the fiber sunk in a cylinder containing Sample A fiber that has been drained of deionized water.

A review of the fiber lengths and apparent densities of chicken feather fibers studied by Hong and Wool [2005] and Barone and Schmidt [2005] suggests that there is a correlation between fiber length and apparent density. While Hong and Wool reported a typical fiber length of 8 mm and an apparent density of 0.8, Schmidt and Baron reported fiber lengths as short as 3.2 mm and an apparent density of 0.89. This trend agrees with this study's apparent specific gravity results for fiber. Sample A fiber was found to have a much shorter average length of 0.6 mm and a much greater apparent specific gravity of 1.2. This suggests that apparent specific gravity results increase with decreasing fiber length. The hollows, or voids, inside chicken feather fibers may become more accessible to the ethanol (used in this study and by Barone and Schmidt [2005]) or polymeric resin (used by Wool [2005]), used to measure apparent specific gravity, as fiber length decreases. For a fiber of some critical length, the void inside of this fiber would act as a part of its surface, and as a result only the solid matter of this fiber would be accounted for by a measurement of apparent density. Again assuming a density of 1.3 g/cm^3 [Arai

et al., 1989] for the solid matter of chicken feather fiber, apparent specific gravity results would approach 1.3 g/cm^3 with decreasing fiber length. This would account for the various apparent specific gravity and apparent density results obtained for chicken feather fiber.

The same trend would be expected to apply to inner quill, which is porous. For a quill particle of some critical length, the void inside of this particle would act as a part of its surface, and as a result only the solid matter of this quill particle would be accounted for by a measurement of apparent density.

If apparent specific gravity measurements conducted in this manner are a function of the degree to which voids are infiltrated by ethanol, then it follows that results could be influenced by vacuum pressure during degassing. Higher vacuum pressures could cause air occupying voids to escape and be replaced by ethanol during degassing. However, results showed that this did not occur. Measurements of Sample A fiber apparent specific gravity were approximately the same at 0, 36, and 57 cm Hg vacuum pressure. At 0 cm Hg, the standard deviation of measurements increased. These results are shown in Figure 4.8.

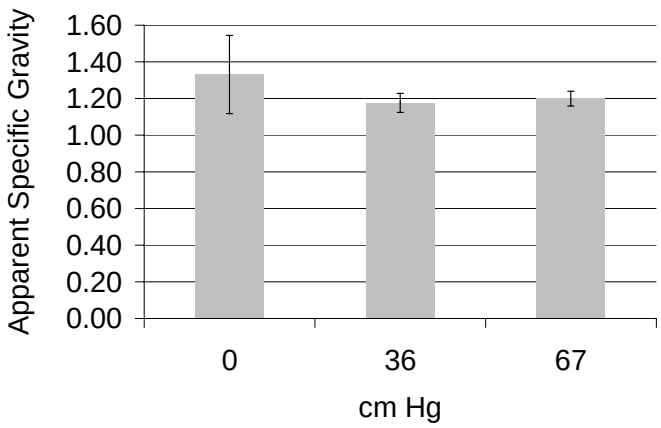

Figure 4.8 Apparent specific gravities of Sample A fiber degassed at 0, 36, and 67 cm Hg vacuum pressure.

4.1.4 Chemical Durability

The chemical durability of Sample A fiber and quill was measured as mass loss over time of replicate samples stored in solutions of dilute acetic acid, saturated gypsum, and concentrated sodium hydroxide. These solutions were tailored to replicate conditions in wood, gypsum, and cement-based composites. Results were compared with those for control samples, CFM stored in deionized water. Tables 4.2 and 4.3 list percent mass loss results.

Table 4.2 Percent mass loss of Sample A fiber in deionized water, a saturated gypsum solution, a dilute acetic acid solution, and a 0.7M NaOH solution.

Solution	0 Days	7 Days	28 Days	56 Days	90 Days	120 Days
Water	14% (5%)	15% (1%)	20% (0.3%)	16% (1%)	14% (0.4%)	16% (7%)
Gypsum		16% (1%)	19% (1%)	17% (1%)	14% (0.1%)	18% (4%)
Acetic		15% (0.3%)	20% (0.2%)	17% (1%)	15% (1%)	16% (4%)
NaOH		100% (0.4%)				

Table 4.3 Percent mass loss of Sample A quill in deionized water, a saturated gypsum solution, a dilute acetic acid solution, and a 0.7M NaOH solution.

Solution	0 Days	7 Days	28 Days	56 Days	90 Days	120 Days
Water	12% (4%)	13% (0.3%)	14% (1%)	13% (1%)	11% (0.2%)	8% (1%)
Gypsum		13% (1%)	14% (0.3%)	11% (1%)	11% (0.4%)	7% (5%)
Acetic		13% (0.4%)	15% (0.3%)	13% (0.3%)	11% (0.4%)	8% (1%)
NaOH		101% (0.1%)				

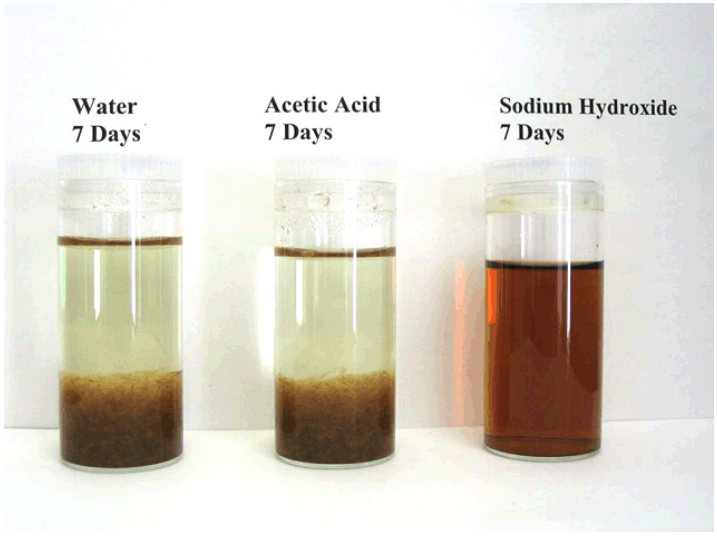

Figure 4.9 Sample D in deionized water, a dilute acetic acid solution, and a 0.7M NaOH solution after 7 days. Almost all solid matter had dissolved in the NaOH solution after 7 days. The brown color of the chicken feather fiber was apparent prior to its exposure and was a result of oven-drying.

CFM stored in concentrated sodium hydroxide (0.7M NaOH) were found to have rapidly degraded. Figure 4.9 depicts the degradation of chicken feather fiber exposed to concentrated sodium hydroxide for 7 days. By 7 days, both Sample A fiber and quill experienced greater than 99% mass loss, indicating that CFM are unstable in strongly alkaline environments. Thus, CFM are incompatible with cement-based materials unless specially treated. These findings are consistent with those of Hamoush and El-Hawary [1994], who examined the effect of chicken feather reinforcement on concrete strength.

Feathers cast in concrete cylinders were found to have severely decayed at the time of testing.

Figure 4.10 shows percent mass loss results relative to results for CFM stored in deionized water. Though the dilute acetic acid and saturated gypsum solutions are clearly not as deleterious to CFM as a concentrated sodium hydroxide solution, results for CFM stored in dilute acetic acid and saturated gypsum solutions are inconclusive. No trend is perceptible, and this is likely due to the low resolution of the data. The standard deviations of individual data points were as great as 7%, which exceeds the highest percent mass loss relative to control data. Thus, it cannot be concluded that CFM would be stable over time in wood and gypsum composites.

Further research is required in order to determine whether CFM would be stable over time in wood and gypsum composites. The same experiment could be repeated using larger sample sizes. A better understanding of optimal oven-drying temperatures would also benefit such a study. Oven-drying caused color changes in the samples, and thus results may have been influenced by property changes in the CFM during oven-drying.

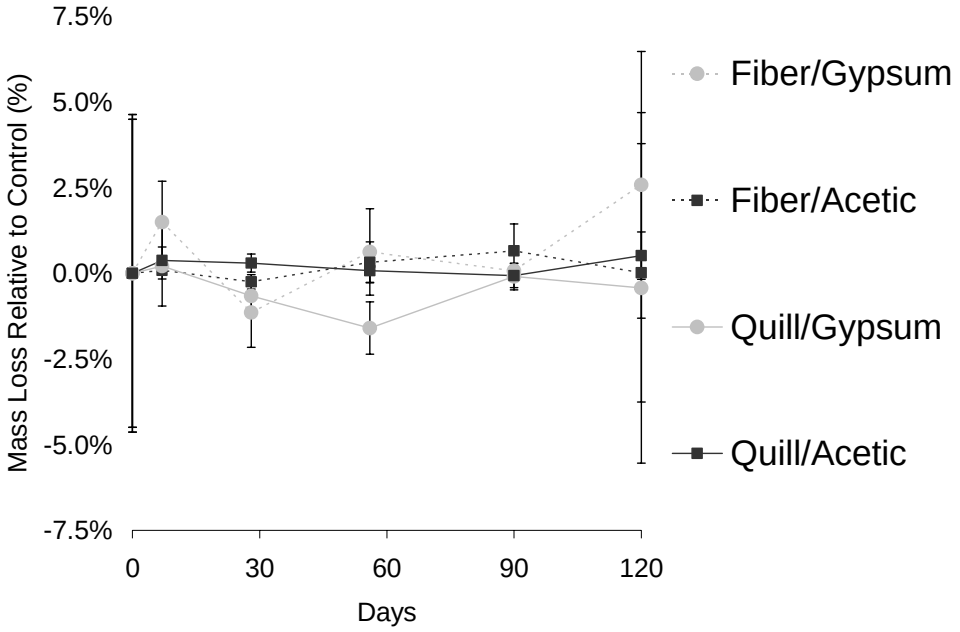

Figure 4.10 Percent mass loss, relative to control samples, of Sample A fiber and quill in a saturated gypsum solution and a dilute acetic acid solution.

4.2 Mechanical Properties

Replicate polyurethane matrix composite coupons containing Sample A fiber, oven-dried fiber, quill, or oven-dried quill (with v_F=0.02, 0.04, or 0.08) were cut from cast sheets. Coupons were tested in uniaxial tension, and composite properties were determined from stress-strain data.

Figure 4.11 illustrates fiber dispersion in fiber and quill coupons. While the particles in the fiber, oven-dried fiber, and quill coupons were found by visual inspection to be well dispersed in the matrix material, the oven-dried quill particles were found to be concentrated along one coupon surface and were therefore not evenly dispersed (Figure 4.22). The surface at which particles were concentrated corresponded to the top surface during casting. This is likely due to the fact that the apparent specific gravity of the oven-dried quill material is less than the specific gravity of the polyurethane matrix

material, 1.1 (reported by the manufacturer). The quill material (conditioned at 50% RH) also has an apparent specific gravity less than 1.1, but it was found to be relatively well-dispersed. Analytical models used to calculate Young's modulus and tensile strength values for CFM assume good fiber dispersion, and the results for oven-dried quill are likely influenced by the fiber dispersion in these coupons. Though concentration of the oven-dried quill occurred, this did not appear to induce any particular fiber orientation.

Visible voids were present in some coupons. Typically, it was coupons with v_F=0.08 which contained visible voids. At this v_F, the high viscosity of the resin-particle mixture limited the effectiveness of degassing.

Figures 4.12 and 4.13 show representative stress-strain curves for fiber and oven-dried fiber coupons relative to neat coupons. The curves are shown terminating at their maximum stress values. Maximum stress values increase with increasing v_F. Values of strain at maximum stress generally decrease with increasing v_F. Figure 4.14 shows a comparison among stress-strain data for fiber, oven-dried fiber, quill, and oven-dried quill coupons with v_F=0.04. The maximum stress of the oven-dried fiber coupon is higher than the maximum stress values of the other coupons, which are approximately equal. Strain at maximum stress is lower for oven-dried fiber and oven-dried quill coupons than for fiber and quill coupons.

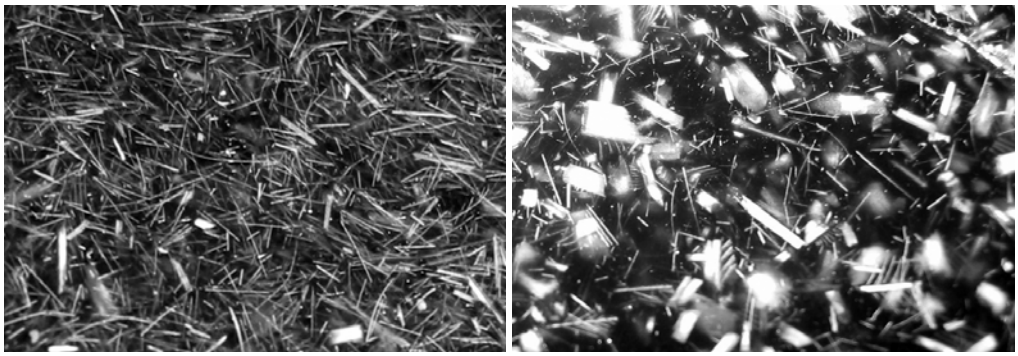

(a) (b)

Figure 4.11 (a) Surface of fiber coupon with v_F =0.08 and (b) surface of quill coupon with v_F =0.04.

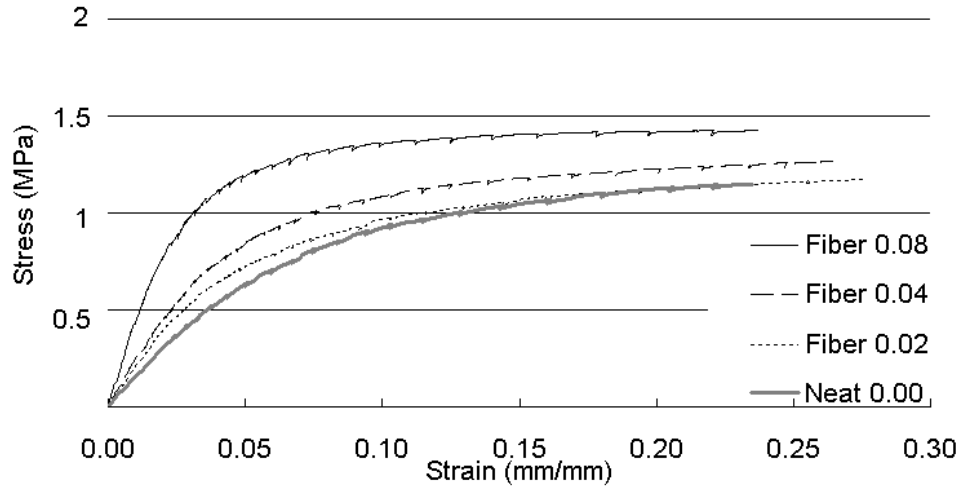

Figure 4.12 Representative stress-strain curves for neat and fiber coupons with v_F = 0.02, 0.04, and 0.08.

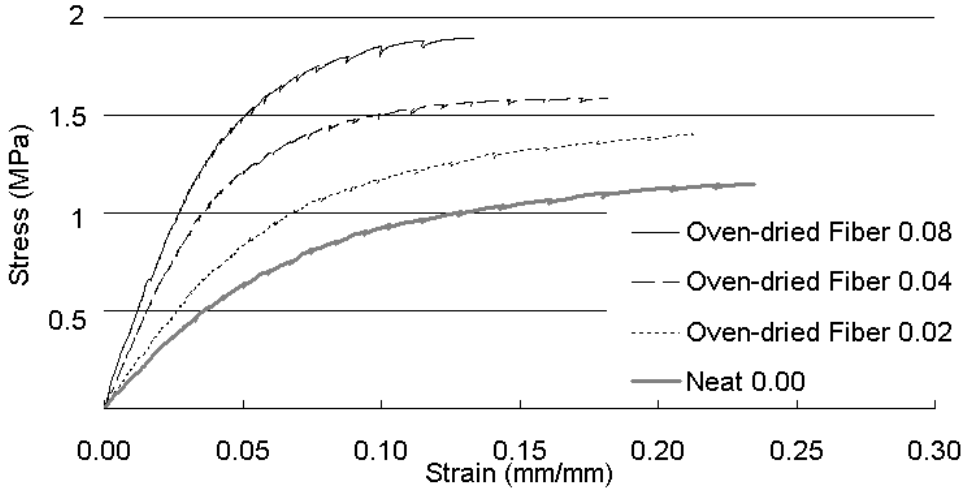

Figure 4.13 Representative stress-strain curves for neat and oven-dried fiber coupons with v_F = 0.02, 0.04, and 0.08.

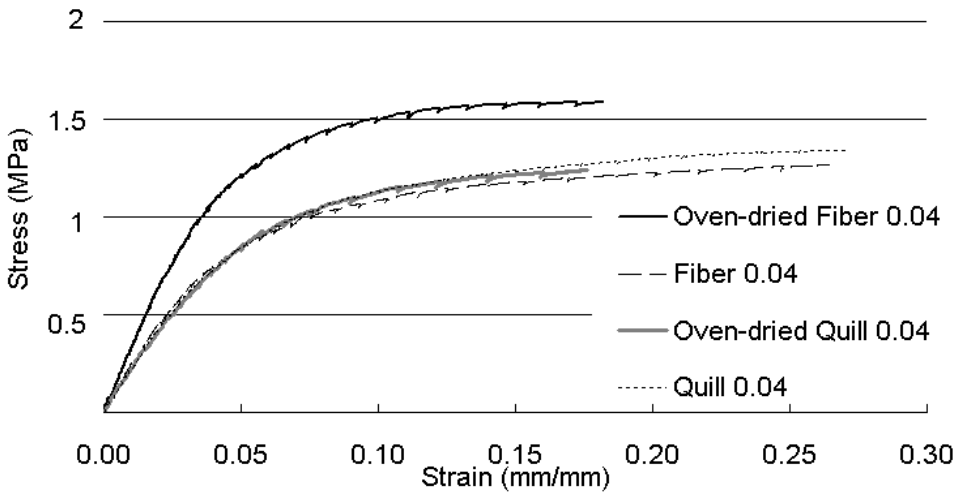

Figure 4.14 Representative stress-strain curves for fiber, oven-dried fiber, quill, and oven-dried quill coupons with v_F = 0.04.

4.2.1 Young's Modulus

Composite Young's modulus, E_C, was determined from stress-strain data in accordance with ASTM E111-04 for replicate coupons containing CFM (Sample A fiber, oven-dried fiber, quill, or oven-dried quill at various v_F), which were tested in uniaxial tension. As expected, the Young's moduli of coupons containing CFM were greater than the Young's moduli of neat coupons, as shown in Figures 4.12 and 4.13 and Table 4.4. The Young's modulus of the neat coupons was 0.016 GPa, which compares favorably with a typical value of 0.025 GPa for polyurethane elastomers [Roylance, 1999]. Figures 4.15, 4.16, 4.18, and 4.19 show that, for fiber and oven-dried fiber coupons, the relationship between v_F and experimental values for E_C is substantially linear, and these values increase together. The standard deviation of E_C increased with increasing v_F, as expected. Coupons with high values of v_F were of less consistent quality than coupons with low values of v_F, due to the difficulty of degassing resin and particle mixtures with high viscosities due to high particle content.

Table 4.4 Average experimentally-derived values of E_C for each sample type.

Type	Ec (GPa)			
	vf=0.00	vf=0.02	vf=0.04	vf=0.08
Fiber	0.016 (0.003)	0.023 (0.001)	0.028 (0.005)	0.037 (0.018)
Oven-dried Fiber	0.016 (0.003)	0.020 (0.005)	0.042 (0.008)	0.053 (0.011)
Quill	0.016 (0.003)	- -	0.021 (0.007)	- -
Oven-dried Quill	0.016 (0.003)	- -	0.026 (0.002)	- -

The average experimentally-derived values of E_C for each sample type were used in Equation 3.3 (rule of mixtures) to calculate the effective Young's moduli, $E_{F-Effective}$, for Sample A fiber, oven-dried fiber, quill, or oven-dried quill. Three particle volume fractions of fiber and oven-dried fiber were examined: v_F=0.02, 0.04, and 0.08. Only one particle volume fraction of quill and oven-dried quill was examined, due to limited sample availability. As is illustrated in Figures 4.15 and 4.16, unique values of $E_{F-Effective}$ were calculated at each v_F. Thus, $E_{F-Effective}$ is reported as a range of values for fiber and oven-dried fiber and as a single value for quill and oven-dried quill in Table 4.5. Calculations yielded 0.3-0.4 GPa for fiber $E_{F-Effective}$ and 0.2-0.7 GPa for oven-dried fiber $E_{F-Effective}$. Higher values for oven-dried fiber may be due to improved particle-matrix interface properties. Also, work by Taylor *et al*. [2004] indicates that the mechanical properties of avian feathers improve with decreasing moisture content.

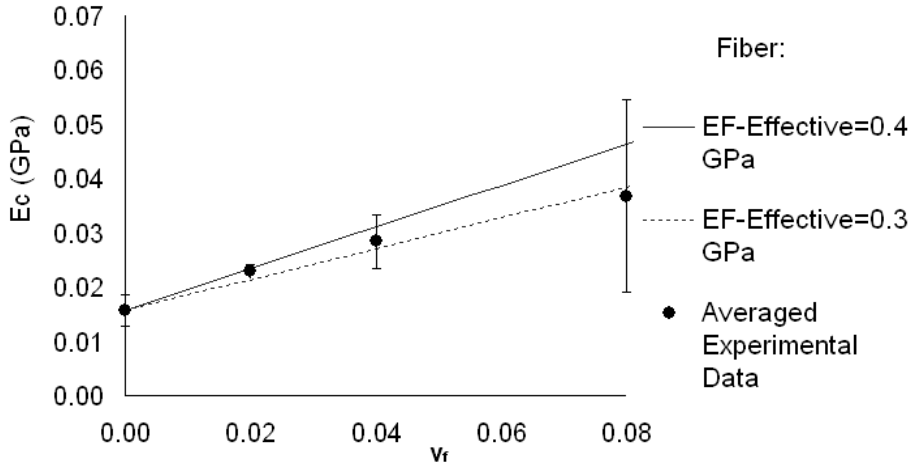

Figure 4.15 Average effective Young's moduli of Sample A fiber coupons and upper and lower bound curves predicted using Equation 2.1 ($E_{F-Effective}$).

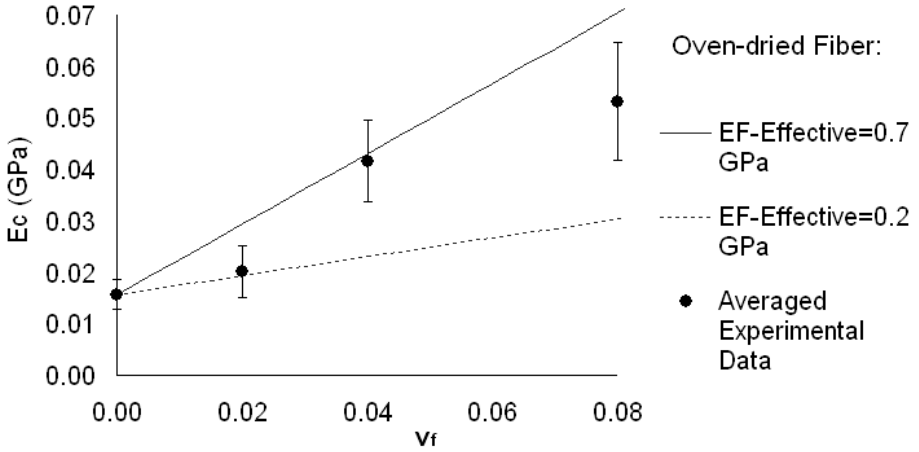

Figure 4.16 Average effective Young's moduli of Sample A oven-dried fiber coupons and upper and lower bound curves predicted using Equation 2.1 ($E_{F-Effective}$).

Table 4.5 Range of calculated values of $E_{F-Effective}$ and E_F for Sample A fiber, oven-dried fiber, quill, and oven-dried quill.

Type	$E_{F-Effective}$ (GPa)	E_F (GPa)
Fiber	0.3 - 0.4	4 - 50
Oven-dried Fiber	0.2 - 0.7	4 - >50
Quill	0.1	3
Oven-dried Quill	0.3	>3

$E_{F-Effective}$ for quill was found to be less than $E_{F-Effective}$ for fiber. Calculation, using Equation 3.3, yielded 0.1 GPa for quill $E_{F-Effective}$ and 0.3 GPa for oven-dried quill $E_{F-Effective}$. It is likely that a higher $E_{F-Effective}$ was determined for oven-dried quill than for quill for the same reasons that a higher $E_{F-Effective}$ was determined for oven-dried fiber than for fiber. Equation 3.4 (Paul model) yielded a value of 0.3 GPa for quill $E_{F-Effective}$ and was not viable for oven-dried quill, due to the asymptotic behavior of the model depicted in Figure 2.12b. The Paul model is incapable of predicting the experimentally-derived value of E_C for oven-dried quill coupons, regardless of the value of $E_{F-Effective}$ for oven-dried quill. The Paul model assumes cubic inclusions and does not consider particle orientation. Thus, it should not necessarily be considered a valid model for the quill material. While the quill fraction does have a lower aspect ratio than the fiber fraction, especially after neglecting particles with diameters less than 30 μm, the particles are not cubic, and thus their orientation cannot necessarily be neglected. Also, the quill particles likely exhibit anisotropy due to the linear nature of feather rachis, especially if full cross sections of rachis (inner quill surrounded by outer quill) remain intact during processing.

For determining $E_{F-Effective}$, Equation 3.3 (rule of mixtures) is preferable to Equation 3.4 (Paul model). $E_{F-Effective}$ for CFM can be assumed to be 0.1-0.7 GPa. This range represents the Young's modulus of a three-dimensional array of particles without accounting for particle orientation or aspect ratio. An array with a different different degree of alignment or aspect ratio distribution would exhibit different properties. Additionally, the fiber-matrix interface properties would likely be different in a different matrix material, and thus the contribution to E_C of a particle array could be affected.

Many factors contribute to sample variability, including chicken size, type, and age, processing regimes, and composite fabrication methods. Due to the high degree of sample variability, it is useful to employ a simplified method for making comparisons among samples which avoids labor-intensive characterization of particle orientation and aspect ratio distribution. Values of $E_{F-Effective}$ form a basis for making simplified comparisons among samples.

In contrast to a calculation of $E_{F-Effective}$ using Equation 3.3 (rule of mixtures), a calculation of particle Young's modulus, E_F, using Equation 2.4 (modified Cox model) accounts for particle aspect ratio and particle alignment. E_F represents the average Young's modulus of a single particle in uniaxial tension. The average experimentally-derived value of E_C for each sample type was used in Equation 2.4 (modified Cox model) to iteratively calculate fiber Young's modulus, E_F, for Sample A fiber, oven-dried fiber, quill, and oven-dried quill. Equation 2.4, with a value for ψ of $1/6$, assumes a three-dimensionally random array of particles. In order to verify that a coupon thickness of 5 mm allows for three-dimensional randomness, replicate coupons containing Sample A fiber (v_F=0.04) with thicknesses of approximately 5, 10, and 15 mm were tested in uniaxial tension, and average values of E_C were compared. If a coupon thickness of 5 mm were not great enough to allow for three-dimensional randomness, then E_C would decrease with increasing thickness, because fibers would then becomes less aligned. However, Figure 4.17 shows that there is no trend as a function of coupon thickness. Given an average particle length of 0.6-0.7 mm and a

maximum particle length of 3.6 mm, it is reasonable that a coupon thickness of 5 mm would allow for three-dimension randomness.

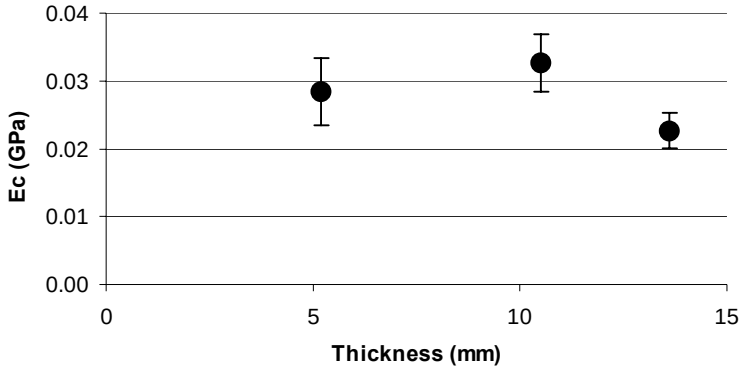

Figure 4.17 Composite Young's modulus as a function of coupon thickness.

As with $E_{F-Effective}$, unique values of E_F were calculated at each v_F. Figure 4.18 illustrates two unique values of E_F (each corresponds to a unique v_F) calculated for Sample A fiber. E_F is reported as a range of values for fiber and oven-dried fiber and as a single value for quill and oven-dried quill in Table 4.5. Calculations yielded 4 - 50 GPa for E_F of fiber and 4 - >50 GPa for E_F of oven-dried fiber. An upper boundary for E_F of oven-dried fiber cannot be calculated using the modified Cox model due to asymptotic behavior similar to that exhibited by the Paul Model and depicted in Figure 2.12b. The modified Cox model is incapable of predicting the experimentally-derived value of E_C for the oven-dried fiber coupons with v_F =0.04 , regardless of the value of E_F for oven-dried fiber. This is likely a result of deviation between the assumptions of the model and the conditions of the experiment. However, because E_C for oven-dried fiber at v_F =0.04 is greater than the curve predicted using Equation 2.4 and a value for E_F of 50 GPa, it can be assumed that the upper boundary of E_F for oven-dried fiber is greater than 50

GPa. Calculation yielded 3 GPa for E_F of quill, while E_F could not be calculated for oven-dried quill due to the asymptotic behavior of the modified Cox model. The modified Cox model is incapable of predicting the experimentally-derived value of E_C for the oven-dried quill coupons, regardless of the value of E_F for oven-dried quill. This is likely a result of deviation between the assumptions of the model and the conditions of the experiment. However, because E_C for oven-dried quill is greater than E_C for quill (Table 4.4), it can be assumed that E_F for oven-dried quill is greater than E_F for quill, or >3 GPa.

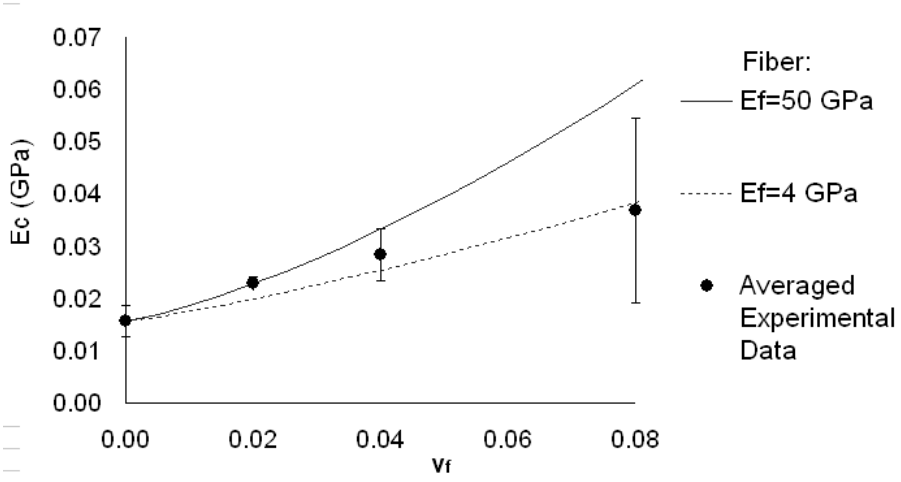

Figure 4.18 Average Young's moduli of Sample A fiber coupons and upper and lower bound curves predicted using Equation 2.4 (E_F).

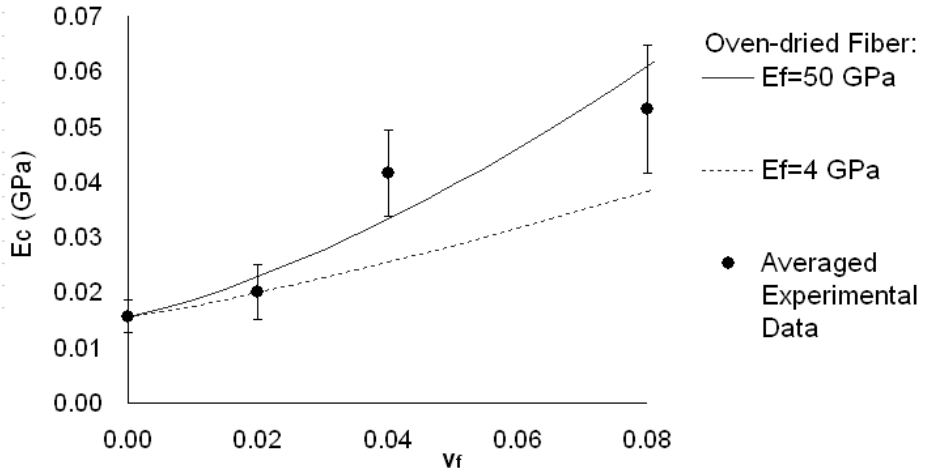

Figure 4.19 Average Young's moduli of Sample A oven-dried fiber coupons, a lower bound curve predicted using Equation 2.4 (E_F), and the upper bound curve for Sample A fiber (Figure 4.18). Equation 2.4 cannot be used to calculate an upper bound curve for Sample A oven-dried fiber. The upper bound curve from Figure 4.18 is shown for the purpose of comparison.

E_F for CFM can be assumed to be 3 - >50 GPa. This value is comparable to the elastic modulus of other natural fibers. As shown in Table 2.2, the elastic moduli of flax and jute are 27 GPa and 55 GPa, respectively [Saheb and Jog, 1999]. Specific modulus is defined by Saheb and Jog [1999] as elastic modulus divided by specific gravity. They show that popular natural fibers have specific moduli (50 GPa for flax and 38 GPa for jute) which are comparable to the specific modulus of glass fiber, 28 GPa. Given specific gravity values of 0.8 for chicken feather quill and 1.1 for chicken feather fiber, CFM can be assumed to have comparable specific moduli.

The included water that differentiates fiber from oven-dried fiber and quill from oven-dried quill can be thought of as void content that does not contribute to composite mechanical properties. Such void content would lower E_C and thus calculated values of $E_{F-Effective}$ and E_F. Values derived from oven-dried particle coupons are therefore considered to be more representative of actual fiber and quill properties. Another

consideration is that the Young's modulus of keratin has been found to vary with moisture content. The Young's modulus of ostrich feather rachis was found by Taylor *et al.* [2004] to more than double when conditioned at 0% RH as opposed to 100% RH. Thus, the higher values of E_C for coupons containing oven-dried particles (Table 4.4) may be partly a function of keratin's increased mechanical properties when moisture has been removed.

Results for quill and oven-dried quill of ≥3 GPa compare favorably with results reported by Taylor *et al.* [2004] for the Young's modulus of ostrich father rachis. Ostrich feathers can be assumed to have mechanical properties similar to those of chicken feathers because both birds are flightless. Taylor *et al.* [2004] reported values between 1 and 4 GPa, with 1 GPa corresponding to rachis conditioned at 100% RH and 4 GPa corresponding to rachis conditioned at 0% RH.

4.2.2 Tensile Strength

Composite tensile strength, σ_C, was determined from stress-strain data for replicate coupons containing CFM (Sample A oven-dried fiber and oven-dried quill at various v_F), which were tested in uniaxial tension. A coupon's tensile strength was taken as its maximum stress. For the purpose of characterizing three-dimensionally random particle array tensile strength, $\sigma_{F-Effective}$, and fiber tensile strength, σ_F, only oven-dried samples were of interest. As previously stated, oven-dried samples are considered to be more representative of actual fiber and quill properties. Also, the tensile strength of ostrich feather rachis was found by Taylor *et al.* [2004] to more than double when conditioned at 0% RH as opposed to 100% RH. Most importantly, an examination of

oven-dried fiber and oven-dried quill coupon fracture surfaces showed that these coupons experienced fiber fracture at failure, while fiber and quill coupons experienced fiber pull-out at failure. Thus, oven-dried fiber and oven-dried quill coupons can be used for the characterization of $\sigma_{F-Effective}$ and σ_F. Fiber and quill coupon behavior was likely controlled by the particle-matrix interface and bond strength, and thus these coupons cannot be used for the characterization of $\sigma_{F-Effective}$ and σ_F. The behavior of the coupons containing oven-dried particles may have been due to the lack of moisture in these samples, which may have increased the strength of the particle-matrix interface in these coupons. Figures 4.20, 4.21, and 4.22 depict fracture surfaces for fiber and quill coupons as well as oven-dried fiber and oven-dried quill coupons.

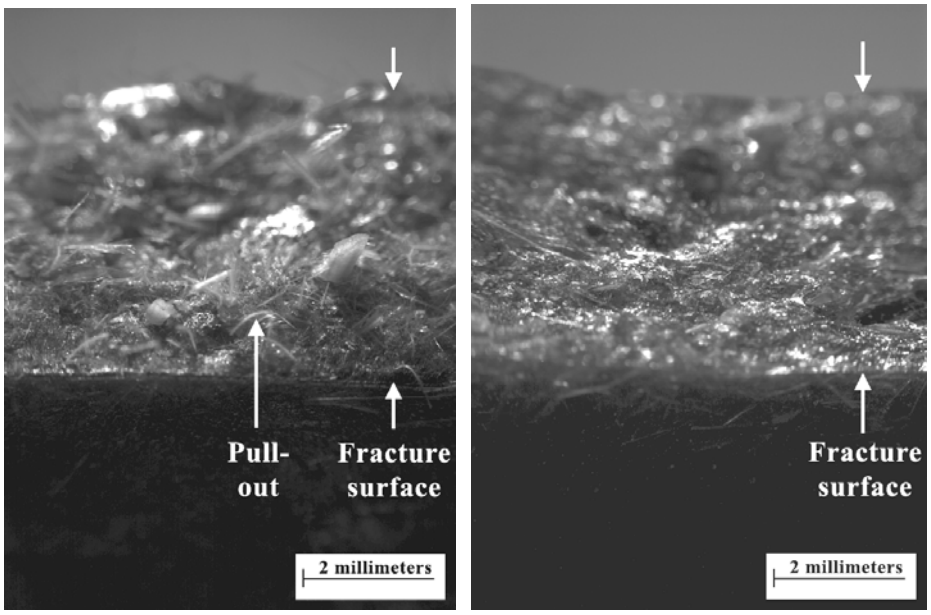

(a) (b)

Figure 4.20 Fracture surface and coupon face of (a) a fiber coupon and (b) an oven-dried fiber coupon with v_F = 0.04. The visible fibers indicate particle pull-out, while the smooth surface of the oven-dried fiber coupon indicates particle fracture.

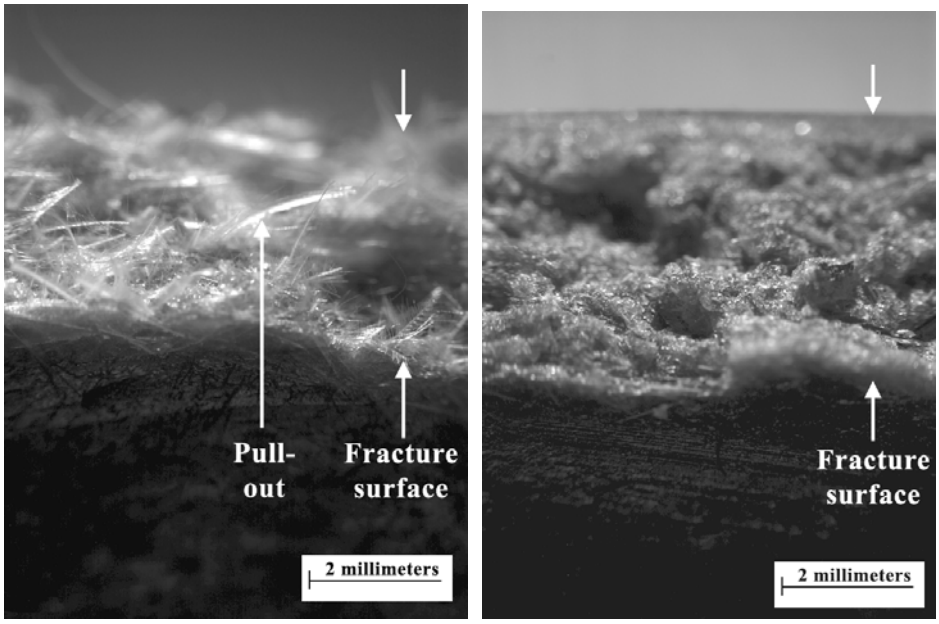

(a) (b)

Figure 4.21 Fracture surface and coupon face of (a) a fiber coupon and (b) an oven-dried fiber coupon with v_F = 0.08. Here, more fibers are visible, and this further indicates particle pull-out. The smooth—though not flat—surface of the oven-dried fiber coupon indicates particle fracture.

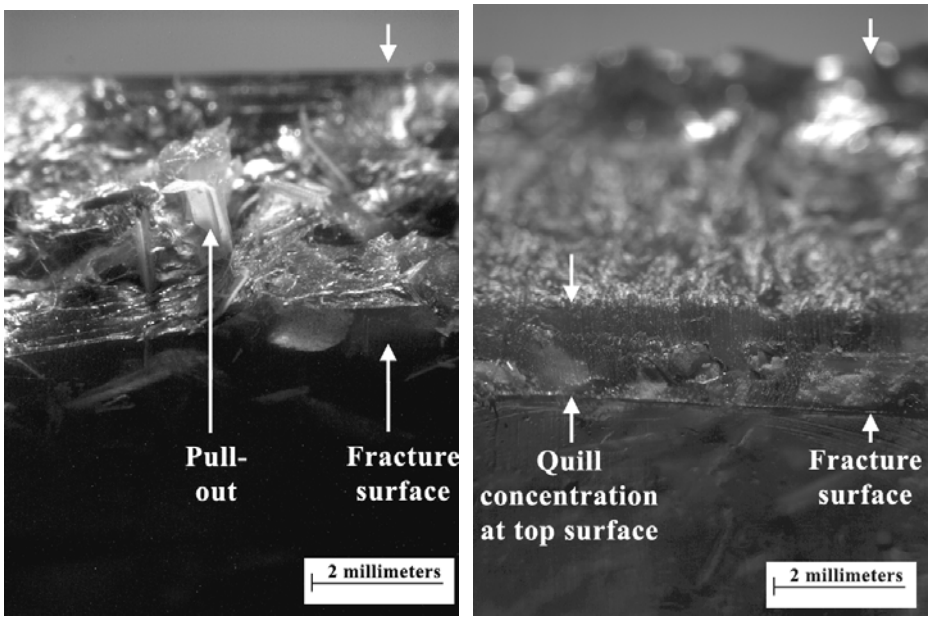

(a) (b)

Figure 4.22 Fracture surface and coupon face of (a) a quill coupon and (b) an oven-dried quill coupon with v_F = 0.04. The visible quill material indicates particle pull-out, while the smooth surface of the oven-dried quill coupon indicates particle fracture. Particles became concentrated at the top surface of the quill coupon during casting.

Table 4.6 Average experimentally-derived value of σ_C for each sample type.

Type	σc (MPa)							
	vf=0.00		vf=0.02		vf=0.04		vf=0.08	
Oven-dried Fiber	1.22	(0.08)	1.34	(0.10)	1.61	(0.02)	1.87	(0.14)
Oven-dried Quill	1.22	(0.08)	-	-	1.24	(0.05)	-	-

As depicted in Table 4.6 and Figure 4.23, σ_C increased, as expected, with increasing volume fractions of Sample A oven-dried fiber. The values of σ_C for oven-dried fiber and oven-dried quill coupons were used in Equation 3.5 (rule of mixtures) to calculate the effective tensile strengths, $\sigma_{F-Effective}$, for Sample A oven-dried fiber and oven-dried quill. Values of $\sigma_{F-Effective}$ for each sample type were averaged. Three particle volume fractions of oven-dried fiber were examined: v_F=0.02, 0.04, and 0.08. Only one particle volume fraction of oven-dried quill was examined, due to limited sample availability. As illustrated in Figure 4.23, unique values of $\sigma_{F-Effective}$ were calculated at each v_F. Thus, $\sigma_{F-Effective}$ is reported as a range of values for oven-dried fiber and as a single value for oven-dried quill in Table 4.7. Calculations yielded 11-13 MPa for oven-dried fiber $\sigma_{F-Effective}$ and 4 MPa for oven-dried quill $\sigma_{F-Effective}$.

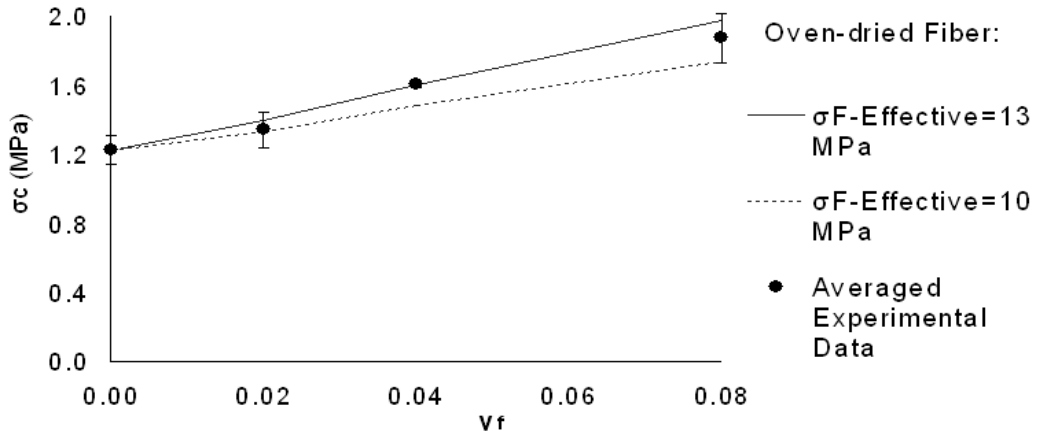

Figure 4.23 Average effective tensile strengths of Sample A oven-dried fiber coupons and upper and lower bound curves predicted using Equation 2.7 ($\sigma_{F-Effective}$).

Table 4.7 Range of calculated values of $\sigma_{F-Effective}$ and σ_F for Sample A oven-dried fiber and oven-dried quill.

Type	$\sigma_{F\text{-}Effective}$ (MPa)	σ_F (MPa)
Oven-dried Fiber	10 - 13	>70
Oven-dried Quill	4	10

$\sigma_{F-Effective}$ for CFM can be assumed to be 4-13 MPa. However, this range represents the tensile strength of a three-dimensional array of particles without accounting for orientation or aspect ratio. An array with a different degree of alignment or aspect ratio distribution would exhibit different properties. Additionally, the fiber-matrix interface properties would likely be different in a different matrix material, and thus the contribution to σ_C of a particle array could be affected.

Many factors contribute to sample variability, including chicken size, type, and age, processing regimes, and composite fabrication methods. Due to the high degree of sample variability, it is useful to employ a simplified method for making comparisons among samples which avoids labor-intensive characterization of particle orientation and

aspect ratio distribution. Values of $\sigma_{F-Effective}$ form a basis for making simplified comparisons among samples.

In contrast to a calculation of $\sigma_{F-Effective}$ using Equation 3.5 (rule of mixtures), a calculation of particle tensile strength, σ_F, using Equation 2.12 (Baxter model) accounts for particle aspect ratio and particle alignment. σ_F represents the average tensile strength of a single particle in uniaxial tension. Equation 2.12 was used to characterize σ_F for Sample A oven-dried fiber and oven-dried quill. Trial values of σ_C were calculated using trial values of σ_F and Equation 2.12. These values of σ_C were compared with the average experimentally-derived value of σ_C for each sample type (Table 4.6). For oven-dried fiber and oven-dried quill, the trail value of σ_F which predicted to the nearest MPa the average experimentally-derived value of σ_C using Equation 2.12 was selected as σ_F.

An important consideration when using Equation 2.12 is the concept of critical aspect ratio, $\left(L/d\right)_c$. Particles of aspect ratio $L/d < \left(L/d\right)_c$ are unable to develop their full tensile strength in a composite. As a result, σ_C of a composite with particles of aspect ratio $L/d < \left(L/d\right)_c$ will be less than that of the same composite with particles of aspect ratio $L/d \geq \left(L/d\right)_c$. The rule of mixtures calculation of $\sigma_{F-Effective}$ gives the properties of a particle array and thus does not consider whether the aspect ratio of the particles is greater or less than $\left(L/d\right)_c$. In the case of the Baxter model, the equation for σ_C is a function of σ_F when $L/d \geq \left(L/d\right)_c$. When $L/d < \left(L/d\right)_c$, σ_C is no longer a function of σ_F.

Thus, a value for σ_F cannot be accurately determined from a composite with particles of aspect ratio $L/d < (L/d)_c$. Because $(L/d)_c$ is directly proportional to σ_F in its defining equation, Equation 2.9, there exists a critical value of σ_F above which $L/d < (L/d)_c$ and Equation 2.12 can no longer be used to determine σ_F. In the case of oven-dried fiber, this value is σ_F=70 MPa. In the case of oven-dried quill, this value is σ_F=40 MPa.

The σ_C calculated using σ_F=70 MPa for oven-dried fiber and Equation 2.12 (Baxter model) under-predicted average experimentally-derived values of σ_C for oven-dried fiber coupons by as much as 29% (for v_F=0.08). Equation 2.12 is unable to yield a higher value of σ_C than that which was calculated using σ_F=70 Mpa, the critical value of σ_F above which $L/d < (L/d)_c$. If the aspect ratio of the particles was greater, then the critical value of σ_F would increase, and a greater value for σ_F would increase the σ_C yielded by the Equation 2.12. It can be assumed that oven-dried fiber σ_F is >70 MPa.

The σ_C calculated using σ_F=12 MPa for oven-dried quill and Equation 2.12 (Baxter model) predicted the average experimentally-derived value of σ_C for oven-dried quill, 1.24 MPa, to the nearest 0.1%. A value of 12 MPa for oven-dried quill σ_F is less than the critical value of σ_F for oven-dried quill, 40 MPa. Thus, it can be assumed that the particles developed their full strength. While this prediction shows excellent agreement with experimental results, 1.24 MPa is approximately equal to the tensile strength of the matrix material, 1.22 MPa. Thus, there is not adequate resolution for a precise characterization of oven-dried quill σ_F using the Baxter model and the

experimentally-derived data. It can be assumed that oven-dried quill σ_F is approximately 10 MPa.

As shown in Table 4.7, σ_F for CFM can be assumed to be 10 - >70 GPa. Results indicate that oven-dried fibers have a higher tensile strength than oven-dried quill. It can be assumed that this relationship applies to fiber and quill as well. The lower tensile strength of the quill may be due to the relative weakness of the outer quill material (quill samples were composed of both inner and outer quill). Outer quill keratin has been shown by Schmidt and Line [1996] to be less ordered and have less cross-linking than fiber and inner quill keratin, and thus be weaker.

Hong and Wool [2005] measured the tensile strength of chicken feather fibers directly and reported strengths of 41-130 MPa. This relatively broad range was reportedly due to the heterogeneity of the fibers. Fiber tensile strength results of 94-187 MPa were calculated from experimentally-derived fracture energy data for feather fiber reinforced composites. Hong and Wool's [2005] range of 94-187 MPa agrees with the results of this study, which predicted a tensile strength of >70 MPa.

CHAPTER V

CONCLUSIONS

5.1 Summary of Results and Recommendations

Key physical properties, including moisture content, aspect ratio, apparent specific gravity, and chemical durability, were determined for processed chicken feather fiber and quill. As well, key mechanical properties, including Young's modulus and tensile strength, were calculated for processed chicken feather fiber and quill.

Though previous studies by Barone and Schmidt [2005], Dweib *et al.* [2004], Hong and Wool [2005], and Kar and Misra [2004] have focused on chicken feather fiber, quill constitutes 5-40% of processed CFM [Kock *et al.*, 2005]. Thus, it is productive to determine the particular assets and liabilities of this material as well. This work has comprehensively studied physical and mechanical properties of both processed fiber and quill. Thus, it adds to current knowledge of the properties of the fiber fraction and provides a foundation of knowledge of properties of the quill fraction. This information will aid in the development of successful high volume applications for both chicken feather fiber and quill.

The moisture content of processed chicken feather quill had not previously been measured. This work indicates that processed fiber and quill contain a similar amount of moisture, 16-20%, after conditioning at 110°C$\pm$3^{o} and 50% RH. Inner and outer quill may behave differently when considered separately.

The aspect ratio of processed chicken feather quill had not previously been measured. This work shows that the quill fraction has a lower aspect ratio than the fiber

fraction, as expected. However, the quill fraction cannot be considered cubic because it has an aspect ratio of approximately 15-30. This work also indicates that different processing regimes can produce CFM with different aspect ratios. The aspect ratios of samples processed by MaXim LLC were 15-50, while the aspect ratios of samples processed by Tyson Foods were greater than 1000, according to Hong and Wool [2005].

It was previously reported that the fiber fraction is lighter than the quill fraction [Gassner *et al*., 1998]. However, this work indicates that the apparent specific gravity of the quill fraction is less than that of the fiber fraction. Thus the quill material, in addition to the fiber material, is a promising candidate for use in composite materials. Both materials exhibit low apparent specific gravity even when compared with natural fibers.

This work also indicates that the variability of fiber fraction apparent specific gravity is much greater than previously reported. The apparent specific gravity of the fiber fraction was shown to be as high as 1.2. Values reported by Hong and Wool [2205] and Barone and Schmidt [2005] were in the range of 0.8-0.9. A comparison of apparent specific gravity results with those reported by Hong and Wool [2005] and Barone and Schmidt [2005] indicate that chicken feather fiber apparent specific gravity results may be influenced by particle length, due to a reduction in contained air voids as particle length decreases. Thus, longer fibers may be used to reduce infiltration of chicken feather fibers by matrix material. The low density and good insulating properties of composites containing CFM could be optimized in this way.

The quill fraction and fiber fraction were found to be similarly affected by storage in a strongly alkaline solution modeled after conditions in cement-based materials.

Results indicate that CFM are not compatible with and should not be used in conjunction with cement-based materials.

While the Young's modulus of feather quill from other birds had previously been studied, the Young's moduli of chicken feather fiber and quill had not previously been measured. Results indicate that the fiber fraction has a greater Young's modulus than the quill fraction. The Young's modulus of CFM, 4 - >50 GPa, is comparable to those of other natural fibers such as flax and jute. The specific modulus of CFM is comparable to those of other natural fibers as well as glass fiber. Thus, CFM should be considered for composite applications which would be suitable for other natural fibers such as flax and jute.

The tensile strength of the quill fraction was not previously measured. Results indicate that the quill fraction is weaker than the fiber fraction. These results support previous work by Schmidt and Line [1996] which concluded from thermal (DSC) data that outer quill, a constituent of the quill fraction, is weaker than the fiber material.

Results indicate that reducing the moisture content of CFM for use in composites benefits composite mechanical properties. Previous studies indicate that keratin mechanical properties are improved by moisture reduction. As well, observations of coupon fracture surfaces indicate that the strength of the particle-matrix interface was improved by using oven-dried CFM. However, benefits due to oven-drying may only apply to certain matrix materials.

The concepts of effective Young's modulus and effective tensile strength were introduced in order to allow simplified comparisons among samples of CFM. Such comparisons would be useful while tailoring CFM procurement and processing methods

for particular composite applications for CFM. Effective Young's modulus and effective tensile strength are measures of the contribution of samples of CFM to composite mechanical properties that don't require laborious characterization of other sample properties. During the initial refinement of CFM procurement and processing methods, a simplified comparison method would be advantageous, due to the high degree of sample variability.

5.2 Future Testing

Observed color changes in CFM during oven-drying may indicate that oven-drying at approximately 110°C causes structural changes or even degradation in the fiber and quill fractions. Optimum methods for obtaining reduced-moisture content CFM or oven-dried CFM should be studied, as it is desirable to use low-moisture content CFM for composite applications. The mechanical properties and durability of CFM after being oven-dried at various temperatures could be studied in order to assess potential structural changes or degradation due to oven-drying. Measurements of thermal hysteresis could contribute to the determination of the optimum moisture-reduction methods.

A comparison of this study's apparent specific gravity results with previously reported values for the apparent density of chicken feather fiber indicates that particle length affects apparent density results. This relationship should be studied in depth by testing sets of chicken feather fibers from a single source that have been sieved or otherwise separated by length. As well, a better understanding of the infiltration of CFM by polymer resins or other potential matrix materials is needed. It is expected that the degree of infiltration by a matrix material increases with decreasing particle length.

Scanning electron microscopy could be used to evaluate the degree to which matrix materials are able to infiltrate the hollows of fibers or pores of inner quill particles with various lengths. The insulating properties and low density of CFM are expected to decrease with a reduction in contained air resulting from matrix material infiltration. As a result, information about matrix material infiltration, as it relates to particle length, will aid in the development of optimized composites which take advantage of the low density and good insulating properties of CFM.

The observation that quill particles generally floated in water, while fibers generally did not, indicates that fraction separation while particles are wet may be possible. Some chicken processing plants divert feathers to offal trucks in troughs of water. Energy is consumed to dry saturated feathers before they may be separated in the manner developed by Schmidt and the USDA [Gassner *et al*., 1998]. It may be advantageous, in terms of energy consumption and processing costs, to grind and separate fractions without first drying the feathers. Wet fibers could be wet-laid into fiber mats directly, without previously being dried. The energy and cost benefits of such a process could be studied and compared with alternative methods for obtaining fiber mats.

Chemical durability results indicate that CFM may be compatible with wood-based and gypsum-based composites. However, further testing should be performed to verify these results. A similar study of chemical durability using much greater sample sizes may provide better resolution and allow more precise conclusions to be drawn. The biological durability of CFM should also be studied. Variables including moisture content and temperature are expected to affect the biological durability of CFM. Both long-term biological durability and short-term effects of various moisture contents and temperatures prior to processing should be studied.

Tensile strength results indicated that the aspect ratio of fiber fraction particles was too low to allow for a precise characterization of their tensile strength, σ_F, using Equation 2.12 (Baxter model). Fiber fraction tensile strength should again be characterized using particles with an aspect ratio of at least 130. This is the minimum particle aspect ratio that would allow Equation 2.12 to predict fiber tensile strengths in the range of 94-187 MPa (reported by Hong and Wool [2005]).

Mechanical property calculations assumed, in some cases, that particles were oriented in a three-dimensionally random manner. It is unlikely that particles were oriented in a perfectly random manner, and thus results should be validated. Composites containing fibers of known properties could be tested for the purpose of validating the methods used. As well, composites containing air-laid or wet-laid CFM mats could be tested, and mechanical properties could be calculated with an assumption of two-dimensional randomness. Similar results for particle Young's modulus, E_F, and particle tensile strength, σ_F, would validate this study's results. Additionally, the methods proposed here for calculating particle mechanical properties could be applied to previous experimental work in the literature on composites containing CFM. These results could also be used to validate this study's results.

REFERENCES

Alberts, B., Bray, D., Lewis, J., Raff, M., Roberts, K., Watson, J.D. (1994). *Molecular Biology of the Cell, 3rd Edition*. Garland Press. New York, NY.

Al-Asheh, S. et al. (2003) "Beneficial Reuse of Chicken Feathers in Removal of Heavy Metals from Wastewater," *Journal of Cleaner Production*, 11: 321-326.

Arai, K., Sasaki, N., Naito, S., Takahashi, T. (1989) Crosslinking Structure of Keratin. I. Determination of the Number of Crosslinks in Hair and Wool Keratins from Mechanical Properties of the Swollen Fiber. *Journal of Applied Polymer Science*. 38:1159-1172.

Anatomy. *Chicken Chronicles*. Retrieved March 20, 2004 from http://groups.msn.com/CHICKENCHRONICLES/anatomy.msnw.

ASTM C128-04a. 2004. "Standard Test Method for Density, Relative Density (Specific Gravity), and Absorption of Fine Aggregate," American Society for Testing and Materials, ASTM International.

ASTM D638-03. 2003. "Standard Test Method for Tensile Properties of Plastics," American Society for Testing and Materials, ASTM International.

ASTM E111-04. 2004. "Standard Test Method for Young's Modulus, Tangent Modulus, and Chord Modulus," American Society for Testing and Materials, ASTM International.

Barrodale, Amie (2000). Interview with Walter Schmidt, *McSweeney's,* Last accessed November 29, 2005 at http://www.mcsweeneys.net/2000/06/19schmidt.html

Baxter, W.J. 1998. "The Correct Interpretation of the Tensile Strength of Short Fibre-Reinforced Composites*," Journal of Materials Science*, 33: 5703-5706.

Barnes, P. (2002). Faster Chips With Chicken Feathers. *Tech TV*. Retrieved April 1, 2004 from http://www.techtv.com/news/computing/story/0,24195,3393143,00.html

Barone, J.R. and Schmidt, W.F. (2005) Polyethylene Reinforced with Keratin Fibers Obtained from Chicken Feathers. *Composites Science and Technology*. 65:1173-181.

Bartels, T. (2003). Variations in the morphology, distribution, and arrangement of feathers in domesticated birds. *Journal of Experimental Zoology (Mol. Dev. Evol.)*, 298B: 91-108.

Benmokrane, B., Rahman, H., Ton-That, M.T., and Robert, J.F. (1998) "Improvement of the Durability of FRP Reinforcements for Concrete Structures," *Proceedings of the First International Conference on the Durability of Composites for Construction*, pp. 571-586.

Bonser, R.H.C. and Purslow, P.P. (1995). The Young's modulus of feather keratin. *Journal of Experimental Biology*, 198: 1029-1033.

Bootle, K.R. (1983). Wood in Australia. McGraw-Hill: Sydney.

Cameron, G.J., Wess, T.J., Bonser, R.H.C. (2003). Young's modulus varies with differential orientation of keratin in feathers. *Journal of Structural Biology*, 143: 118–123.

Christensen, R.M. and Waals, F.M. (1972). Effective Stiffness of Randomly Oriented Fibre Composites. Journal of Composite Materials, 6: 518.

Cox, H.L. (1951). The Elasticity and Strength of Paper and Other Fibrous Materials. British Journal of Applied Physics, Vol. 3:72-79.

Das, A.A., Clegg, A.J., Zantout, B., Yakaub, M.M. (1988) "Cast Reinforced Metal Composites" *American Society of Metals*, p. 139.

Durham, S. (2002). Save a Tree, Use Some Feathers. *Agricultural Research Service*. Retrieved March 30, 2004 from http://www.ars.usda.gov/is/pr/2002/020329.htm.

Dweib, M.A., Bullions, T.A., Loos, A.C., Wool, R.P. (2004). Recycled Newspaper and Chicken Feathers as Reinforcement Fiber in Bio-composite Materials. *ANTEC 2004 International Conference Proceedings*, p1478-1481.

Dweib, M.A., Hu, B., O'Donnell, A., Shenton, H.W., Wool, R.P. (2003). All natural composite sandwich beams for structural applications. *Composite Structures*, 63: 147–157.

European Parliament (2004). Enjoy your meal! European Parliament in Action Highlights 1999-2004, April 2.

FDA (Food and Drug Administration) (2004). FDA and USDA Request Comments and Scientific Information on Possible New BSE Safeguards, Center for Veterinary Medicine Update, July 9; last accessed January 12, 2005 at www.fda.gov/cvm/index/updates/BSEANPRM.htm.

Feughelman, M. (2002). Natural protein fibers. *Journal of Applied Polymer Science*, 83: 489-507.

Folkes, M.J. (1982). Short Fibre Reinforced Thermoplastics. John Wiley & Sons, Ltd.: England.

Fraser, R.D.B. and Parry, D.A.D. (1996). The molecular structure of reptilian keratin. *International Journal of Biological Macromolecules*, 19: 207-211.

Fraser, R.D.B. and MacRae, T.P. (1980) Molecular Structure and Mechnical Properties of Keratins. *Proceedings of the Symposia of the Society for Experimental Biology Number 34*. p211-246.

Gassner III, G., Schmidt, W.F., Line, M.J., Thomas, C., Waters, R.M. (1998). Fiber and Fiber Products Produced from Feathers. United States Patent # 5705030.

Gentry, T.R. 2001. "Life Assessment of Glass-Fiber Reinforced Composites in Portland Cement Concrete," presented at the 16th Annual Meeting of the American Society for Composites, Blacksburg, Virginia, September 10-12, 2001.

Gentry, R., Kurtis, K., Nanko, H. (2004). Development of Value-Added Products from Chicken Feathers: Paper, Wood Products, and Building Materials. TIP3 Proposal.

GEP (Georgia Environmental Partnership) (2000). Strategies for Biosolids Utilization. Characterization and Quantification of Georgia's Municipal Biosolids Production and Disposal. Last accessed November 28, 2005 at http://www.engr.uga.edu/service/outreach/Biosolids%20Characterization.htm

George, B.R., Bockarie, A., McBride, H., Hoppy, D., Scutti, A. (2003a). Utilization of turkey feather fibers in non-woven erosion control fabrics. *International Non-wovens Journal*, Summer 2003: 45-52.

George, B.R., Bockarie, A., McBride, H., Hoppy, D., Scutti, A. (2003b). Keratin Fiber Nonwovens for Erosion Control. *Natural Fibers, Plastics, and Composites – Recent Advances*. Kluwer Academic Publishers. p67-81.

Gibson, R.F. (1994). Principles of Composite Material Mechanics. McGraw-Hill, Inc. 67-77.

Goettler, L.A. and Cole, W.F. (2001). "Short Fiber-Filled Rubber Composites," *Handbook of Elastomers.* Marcel Dekker, Inc.: New York.

Griffith, B.A. 2002. "Feather Processing Method and Product," United States Patent Application No. 20020079074.

Hamoush, S.A., El-Hawary, M.M. (1994). Feather fiber reinforced concrete. *Concrete International*, 16(6): 33-35.

Hong, C.K., Wool, R.P. (2005). Development of Bio-Based Composite Materials from Soybean Oil and Keratin Fibers. *Journal of Applied Polymer Science*, 95: 1524-1538.

Jacobson, L. (2002, July 8). Can Computers Fly on the Wings of a Chicken? *The Washington Post*. Retrieved April 4, 2004 from http://www.washingtonpost.com/ac2/wp-dyn/A36816-2002Jul7.

Johnson, W.S., Birt, M.J. (1991). Comparison of Some Micromechanics Models for Discontinuously Reinforced Metal Matrix Composites, Journal of Composites Technology & Research. 13:3, 161-167.

Jones, C.C. and Wawner, F.E. (1989) "Fundamental Relationships between Microstructures and Mechnical Properties of Metal Matrix Composites" *The Minerals, Metals, and Materials Society*, p. 47.

Kar, P. and Misra, M. (2004). Use of Keratin Fiber for Separation of Heavy Metals from Water, Journal of Chemical Technology and Biotechnology, 79: 1313-1319.

Katsuki, F. and Uomoto, T. (1995) "Prediction of Deterioration of FRP Rods due to Alkali Attack," *Proceedings, Non-Metallic (FRP) Reinforcements for Concrete Structures*, p82-86.

Kelly, A. and Tyson, W.R. (1965). Tensile Properties of Fibre-Reinforced Metals: Copper/Tungsten and Copper/Molybdenum, *Journal of the Mechanics and Physics of Solid*s, 13: 329-350.

Kock, J.W., Barbieri, R.J., Justice, J.M., Kurtis, K.E., Gentry, T.R., Nanko, H. (2005) "Characterization of Chicken Feather Materials for Use in Biocomposites," Proceedings of the American Society for Composites: Twentieth Technical Conference, Philadelphia, PA, September 7-9, 2005. American Society for Composites, CD-ROM – 15 pp.

Lederer, R. "Integument, Feathers, and Molt," *Ornithology: The Science of Birds*, http://www.ornithology.com/lectures/Feathers.html, accessed 6/23/05.

McGovern, Victoria (2000). "Recycling Poultry Feathers: More Bang For The Cluck" *Environmental Health Perspectives*, August

Mehta, P. K. and P. J. M. Monteiro (2006). Concrete: Microstructure, Properties, and Materials. Third Edition. McGraw-Hill, New York.

Misra, M., Kar, P., Priyadarshan, G., Licata, C. (2001). Keratin protein nano-fiber for removal of heavy metals and contaminants. *MRS Symposium Fall 2001 Proceedings*, 702(U1): 1-7.

Morimoto, H., Ohuchi, K., Minamide, T. (1987) Proceedings of Conference Sintering, Vol. 2: 1344.

Naresh, M.D., Subramanian, V., Arumugam, V., Sanjeevi, R. (1991). "A Study on the Mechanism of Failure in Keratin," *Colloid & Polymer Science*, 269:590-594.

Negri, A., H. Cornell, D. Rivett. 1993. "A Model for the Surface of Keratin Fibers," *Textile Research Journal*, 63(2):109-115.

Paul, B. (1960) Prediction of Elastic Constants for Multiphase Materials. *Transactions of the Metallurgical Society of AIME*, p36-41.

Purslow, P.P. and Vincent, J.F.V. (1978) Mechanical Properties of Primary Feathers from the Pigeon. Journal of Experimental Biology. 72:251-260.

Roylance, D. (1999) Material Properties. http://ocw.mit.edu/NR/rdonlyres/Materials-Science-and-Engineering/3-11Mechanics-of-MaterialsFall1999/698ECA59-8F00-46CC-96A1-B9365CBD63E3/0/props.pdf, accessed 12/7/05.

Saheb, D.N. and J.P. Jog. 1999. "Natural Fiber Polymer Composities: A Review," *Advances in Polymer Technology*, 18(4):351-363.

Schmidt, W.F. (1998). Innovative Feather Utilization Strategies. *1998 National Poultry Waste Management Symposium Proceedings.*

Schmidt, W.F. and Jayasundera, S. (2003) Microcrystalline Keratin Fiber. *Natural Fibers, Plastics, and Composites – Recent Advances*. Kluwer Academic Publishers, p51-66.

Schmidt, W.F. and Line, M.J. (1996). Physical and chemical structures of poultry feather fiber fractions in fiber process development. *1996 Nonwovens Conference TAPPI Proceedings*: 135-141.

Schrooyen, P. (1999a). Structure and properties of feather keratins. *Feather Keratins: Modification and Film Formation,* Chapter 2: 5-22.

Schrooyen, P. (1999b). Thermal and mechanical properties of films from partially carboxymethylated feather keratins. *Feather Keratins: Modification and Film Formation,* Chapter 7: 111-136.

Taylor, A.M., Bonser, R.H.C., Farrent, J.W. (2004). The Influence of Hydration on the Tensile and Compressive Properties of Avian Keratinous Tissues. Journal of Materials Science. 39:939-942.

Tibbetts, G.G., McHugh, J.J. (1999). Mechanical Properties of Vapor-Grown Carbon Fiber Composites with Thermoplastic Matrices. Journal of Materials Research. 14:7, 2871-2880.

Winandy, J.E., J.H. Muehl, J.A. Micales, A. Raina, W. Schmidt. (2003). "Potential of Chicken Feather Fiber in Wood MDF Composites," *Proceedings EcoComp 2003*, P20:1-6.

Wool, R. Personal Communication. September 8, 2005.

Wool, R. and Hong, C. (2004) Low Dielectric Constant Materials from Plant Oils and Chicken Feathers. United States Patent Application Number 20040072976.

Ye, W. and Broughton, R.M. (1999). "Chicken Feather as a Fiber Source for Nonwoven Insulation" International Nonwovens Journal , 8:1, 53-59.

Yu, M., Wu, P., Widelitz, R.B., Chuong, C. (2002). The morphogenesis of feathers. *Nature*, 420: 308-312.